STANFORD UNIVERSITY

DOCTORAL THESIS

Randomized classification: theory and applications

Author:
Charles ZHENG

Supervisor:
Dr. Trevor HASTIE and Dr.
Jonathan TAYLOR

A thesis submitted in fulfillment of the requirements
for the degree of Doctor of Philosophy

in the

Department of Statistics

March 22, 2017

Declaration of Authorship

I, Charles ZHENG, declare that this thesis titled, "Randomized classification: theory and applications" and the work presented in it are my own. I confirm that:

- This work was done wholly or mainly while in candidature for a research degree at this University.

- Where any part of this thesis has previously been submitted for a degree or any other qualification at this University or any other institution, this has been clearly stated.

- Where I have consulted the published work of others, this is always clearly attributed.

- Where I have quoted from the work of others, the source is always given. With the exception of such quotations, this thesis is entirely my own work.

- I have acknowledged all main sources of help.

- Where the thesis is based on work done by myself jointly with others, I have made clear exactly what was done by others and what I have contributed myself.

Signed:

_____

Date:

_____

Stanford University

Abstract

Faculty Name
Department of Statistics

Doctor of Philosophy

Randomized classification: theory and applications

by Charles ZHENG

The Thesis Abstract is written here (and usually kept to just this page). The page is kept centered vertically so can expand into the blank space above the title too...

Acknowledgements

The acknowledgments and the people to thank go here, don't forget to include your project advisor...

Contents

Chapter 1

Introduction

1.1 Recognition tasks

The study of human intelligence, and the study of artificial intelligence, form two major intertwining areas of modern research. The attempt to algorithmically mimic or exceed human perceptual and cognitive capabilities not only advances the application of artificial intelligence for industrial applications, but also sheds light on the nature of biological intelligence, and the nature of intelligence in general. One of the key capabilities of an intelligent system, natural or artificial, is the ability to recognize objects, agents, and signs in the environment based on input data. Human brains have a remarkable ability to recognize objects, faces, spoken syllables and words, and written symbols or words, and this recognition ability is essential for everyday life. While researchers in artificial intelligence have attempted to meet human benchmarks for these classical recognition tasks for the last X decades, only very recent advances in machine learning, such as deep neural networks, have allowed algorithmic recognition algorithms to approach or exceed human performance [CITE].

Within the statistics and machine learning literature, the usual formalism for studying a recognition task is to pose it as a *multi-class classification* problem. One delineates a finite set of distinct entities which are to be recognized and distinguished, which is the *label set* $\mathcal{Y}$. The input data is assumed to take the form of a finite-dimensional real *feature vector* $X \in \mathbb{R}^p$. Each input instance is associated with exactly one true label $Y \in \mathcal{Y}$. The solution to the classification problem takes the form of an algorithmically implemented *classification rule* h that maps vectors X to predicted labels $\hat{Y} \in \mathcal{Y}$. The classification rule can be constructed in a data-dependent way: that is, one collects a number of labelled *training observations* (X_1, Y_1) which is used to inform the construction of the classification rule h. The success of the classification rule h is measured by the *expected loss* or *risk*, which in the case of zero-one loss takes the form

$$\text{Risk}_{0-1}(h) = \Pr[h(X) \neq Y],$$

where the probability is defined with reference to the unknown population joint distribution of (X, Y). A common approach for constructing a classifier h is *empirical risk minimization* [CITE], which constructs h by minimizing the objective function

$$\text{EmpiricalRisk}_{h \in \mathcal{H}}(h) = \frac{1}{n} \sum_{i=1}^{n} I(h(X) \neq Y)$$

where $\mathcal{H}$ is some pre-specified function class.

However, a limitation of the usual multi-class classification framework for studying recognition problems is the assumption that the label set $\mathcal{Y}$ is finite and known in

advance. When considering human recognition capabilities, it is clear that this is not the case. Our ability to recognize faces is not limited to some pre-defined, fixed set of faces; same with our ability to recognize objects in the environment. Humans learn to recognize novel faces and objects on a daily basis. And, if artificial intelligence is to fully match the human capability for recognition, it must also possess the ability to add new categories of entities to its label set over time; however, at present, there currently exists a void in the machine learning literature on the subject of the online learning of new classes in the data [CITE].

The central theme of this thesis is the study of *randomized classification*, which can be motivated as an extension of the classical multi-class classification framework to accommodate the possibility of growing or infinite label sets $\mathcal{Y}$. The basic approach taken is to assume an infinite or even continuous label space $\mathcal{Y}$, and then to study the problem of classification on finite label sets S which are randomly sampled from $\mathcal{Y}$. This, therefore defines a *randomized classification* problem where the label set is finite but may vary from instance to instance. One can then proceed to answer questions about the variability of the performance due to randomness in the labels, or how performance changes depending on the size of the random label set.

An additional set of applications of the randomized classification framework lies in its connection to information theory. Randomized classification is the natural analogue of the *random code* models first studied by Claude Shannon. Furthermore, it becomes possible to prove extensions of Fano's inequality to the case of continuous X and Y by means of randomized classification. Therefore, randomized classification can be used as a means of inferring mutual information.

The rest of the thesis is organized as follows. The remaining sections in this chapter deal with background material on supervised learning and information theory, as well as the application of both to neuroscience, which forms a major motivation for the current work. Chapter 2 introduces the concept of randomized classification, and also establishes some variability bounds which will be used later in the development of inference procedures. Chapter 3 studies the dependence of classification accuracy on the label set size in randomized classification, and a practical method for predicting the accuracy-versus-label set size curve from real data. Chapter 4 and 5 deal with the applications of randomized classification to the estimation of mutual information in continuous data: chapter 4 derives a lower confidence bound for mutual information under very weak assumptions, while chapter 5 works within an asymptotic high-dimensional framework which leads to a more powerful but less robust estimator estimate of mutual information.

1.2   Information and Discrimination

In studying the problem of recognition, we make use of two closely related frameworks: firstly, the multi-class classification framework from the statistics and machine learning literature, and secondly, the concepts of information theory. From a broader perspective, this is hardly unusual, since concepts such as entropy, divergence, and mutual information are commonly applied in theoretical statistics and machine learning. Furthermore, information theory, theoretical statistics, and machine learning are based on the same foundation: measure-theoretic probability theory; one could even say that all three disciplines are subfields of applied probability. However, while the three sub-fields may appear very similar from a mathematical perspective, some differences arise if we examine the kinds of intuitions and assumptions that are characteristic of the literature in each area.

A common problem to all three subfields is the inference of some unobserved quantity on the basis of observed quantities. In classical statistics, the problem is to infer an unknown parameter; in supervised learning, the problem is to predict an unobserved label or response Y; in information theory, the problem is to decode a noisy message. Next, the metric for quantifying achievable performance differs between the three disciplines. In classical statistics, one is concerned with the variance of the estimated parameter, or equivalently, the Fisher information. In machine learning, one seeks to minimize (in expectation) a *loss* function which measures the discrepancy between the prediction and the truth. In information theory, one can measure the quality of the noisy channel (and therefore, the resulting achievable accuracy) through the *mutual information $I(X;Y)$* between the sender's encoded message X and the reciever's recieved message Y. If we specialize within machine learning to the study of classification, then we are concerned with accurate *discrimination* of the input X according to labels Y.

The concepts of *information* and *discrimination* are quite distinct from an intuitive standpoint; however, they are linked at a fundamental level. This link can be seen throughout statistics and machine learning, and in the way we think about statistical problems. A statistical hypothesis test is *informative* because it provides evidence that the data behaves according to a certain hypothesis rather than another: it allows us to *discriminate* between two potential possibilities. More generally, a true message contains *information* if it allows the reciever to understand that the world is in a certain state and not another: it conveys the fact that out of two possible sets of world states, that the reciever is in one state rather than another. The formalism of measure-theoretic probability theory provides yet another example of the conceptual link between information and discrimination[1].

Either natural or artificially intelligence recognition systems must rely on input data that is *informative* of the optimal response if they are to achieve reasonable discriminative accuracy. In natural environments, mammals rely on a combination of visual, auditory, and tactile cues to recognize potential threats in the environment. Mammalian brains integrate all of this sensory information in order to make more rapid and reliable decisions. Generally, increased diversity and quality of the available sources of information will lead to more accurate recognition.

This link between the information content of the sensory input and the achievable discrimination accuracy was first formalized by Claude Shannon via the concept of *mutual information.* The mutual information $I(X;Y)$ quantifies the information content that an input X holds abut a target of interest, Y. For instance, in the case of facial identification, the discrimination target Y is a label corresponding to the identity of the person, and X is an image of the individual's face. An image corrupted by noise holds less information, and correspondingly leads to lower classification accuracies.

The discrmination problem that Shannon studied–the *noisy-channel decoding problem*, is extremely similar to the multi-class classification problem, but also features some important differences. A side-by side comparison between the schematics of multi-class classification and the noisy channel problem is displayed in Figure 1.1.

---

[1]Supposing Ω is a probability space defined with respect to a σ-algebra $\mathcal{F}$, we can represent our state of knowledge with a filtration (or sub-σ-algebra) $\mathcal{F}' \subseteq \mathcal{F}$. Complete knowledge (zero uncertainty) is represented by the full σ-algebra: that is, $\mathcal{F}' = \mathcal{F}$. Partial knowledge is represented by a coarser filtration, $\mathcal{F} \subset \mathcal{F}'$. The filtration, of course, indicates that our knowledge is sufficient to *discriminate* the outcome space Ω into a number of finitely or infinitely many categories. The more information we have, (or, the closer we come to complete knowledge of the outcome), the more finely we can discriminate the realized outcomes given by $\omega \in \Omega$.

Multi-class classification   Information Theory

$$\boxed{\begin{array}{c}\text{message}\\M\end{array}}$$

$$\left(\begin{array}{c}\text{encoder}\\g(M)\end{array}\right)$$

$$\boxed{\begin{array}{c}\text{label }Y\end{array}}$$

$$\boxed{\begin{array}{c}\text{encoded}\\\text{message }Y\end{array}}$$

$$\left(\begin{array}{c}\text{distribution}\\F_{X|Y}\end{array}\right)$$

$$\left(\begin{array}{c}\text{noisy}\\\text{channel}\\F_{X|Y}\end{array}\right)$$

$$\boxed{\begin{array}{c}\text{observation}\\X\end{array}}$$

$$\boxed{\begin{array}{c}\text{observation}\\X\end{array}}$$

$$\left(\begin{array}{c}\text{classification}\\\text{rule }h(X)\end{array}\right)$$

$$\left(\begin{array}{c}\text{decoder}\\d(X)\end{array}\right)$$

$$\boxed{\begin{array}{c}\text{estimate }\hat{Y}\end{array}}$$

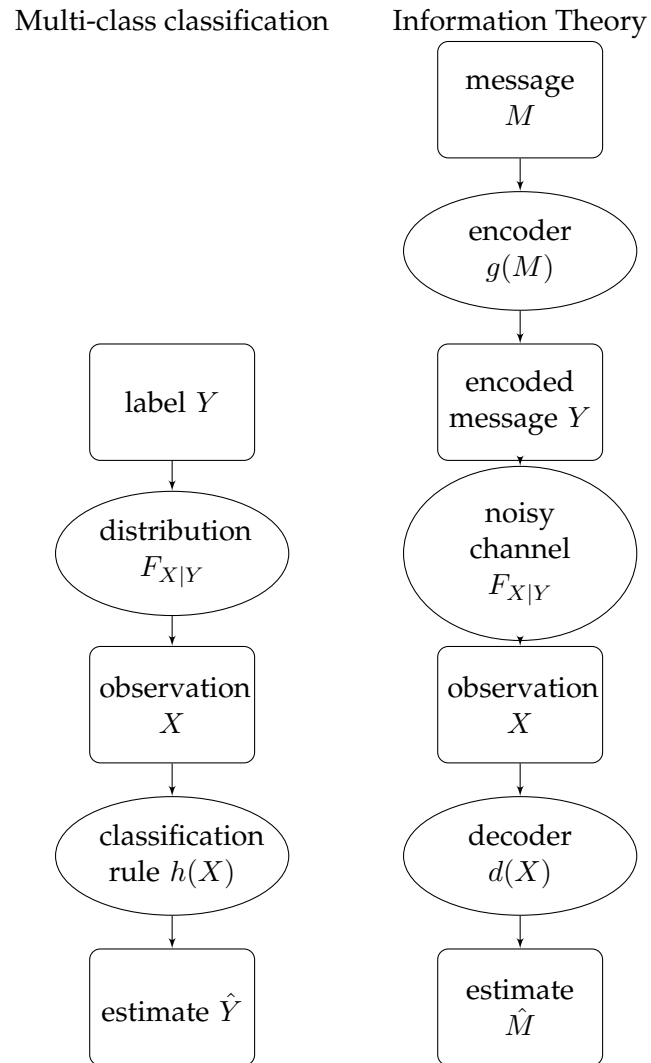$$\boxed{\begin{array}{c}\text{estimate}\\\hat{M}\end{array}}$$

FIGURE 1.1: Comparing the discrimination tasks in multi-class classification and information theory.

We will now review the relevant background for supervised learning and information theory, to give the context for each side of figure 1.1. Afterwards, we will compare and contrast the supervised learning and information theory, and note what kind of cross-talk exists between the two related fields, and what new developments could still arise by way of a dialogue between supervised learning and information theory. One such new development is the *randomized classification* model, since it is a very close analogue of the *random code* model studied in information theory.

1.2.1 Supervised learning

- Supervised learning task is defined using a prediction task.

- 1. A predictive model is learned using training data

- 2. The performance of the model on the prediction task is estimated using independent test data

- Classical examples of prediction tasks: regression and classification

- Third example: identification

- Definition of Bayes prediction model

- General definition of supervised learning task

- SL performance can be a scalar

- SL can be used to test for independence

- Bayes performance satisfies data-processing inequality

- How SL is interpreted in MVPA as information

- Section 3, we'll see how Bayes performance can be legitimately considered a measure of information

In multi-class classification, we may assume without loss of generality that the data has been generated in the following manner:

1. First, a label Y is drawn according to some distribution from the label set $\{y_1, \ldots, y_k\}$.

2. Secondly, the new observation X is drawn according to the unknown conditional distribution $F_{X|Y}$.

3. Finally, an estimated label $\hat{Y} = h(X)$ is obtained according to a data-dependent classification rule, h. Typically, h is determined by fitting a model to training data.

In the particular application, the above description may not match the *causal relationship* between X and Y: however, whether X is drawn conditional on Y, or Y is drawn conditional on X, or that (X, Y) are drawn from some joint distribution, makes no difference from the theoretical standpoint, since only the statistical (and not causal) properties of the joint distribution (X, Y) are relevant for determining the peformance of the classification rule $h(X)$.

1.2.2   Information Theory

Meanwhile, in the noisy channel model, we assume that the sender wants to transmit message M, out of a finite set of possible messages $\mathcal{M} = \{1, \ldots, m\}$. The message must be encoded into a signal $Y \in \mathcal{Y}$, which is sent through a stochastic channel $F_{X|Y}$. Given that a signal y is sent through the channel, the reciever observes a signal X drawn from the distribution $F_{X|y}$. The communications problem is to design an encoding function $g(M)$, which is an injective map from messages $\{1, \ldots, m\}$ to signals in $\mathcal{M}$, and a corresponding decoding function $d(X)$ which infers the message $\{1, \ldots, m\}$ from the recieved signal X.

While Shannon's theory of information was motivated by the problem of designing communications system, the applicability of mutual information was quickly recognized by neuroscientists. Only four years after Shannon's seminal paper in information theory (1948), McKay and McCullough (1952) inaugurated the application of mutual information to neuroscience. If $\boldsymbol{X}$ and $\boldsymbol{Y}$ have joint density $p(\boldsymbol{x}, \boldsymbol{y})$ with respect to the product measure $\mu_x \times \mu_y$, then the mutual information is defined as

$$\mathrm{I}(\boldsymbol{X}; \boldsymbol{Y}) = \int p(\boldsymbol{x}, \boldsymbol{y}) \log \frac{p(\boldsymbol{x}, \boldsymbol{y})}{p(\boldsymbol{x})p(\boldsymbol{y})} d\mu_x(\boldsymbol{x}) d\mu_y(\boldsymbol{y}).$$

where $p(\boldsymbol{x})$ and $p(\boldsymbol{y})$ are the marginal densities with respect to μ_x and μ_y[2]. Since then, mutual information has enjoyed a celebrated position in both experimental and theoretical neuroscience. Experimentally, mutual information has been used to detect strong dependencies between stimulus features and features derived from neural recordings, which can be used to draw conclusions about the kinds of stimuli that a neural subsystem is designed to detect, or to distinguish between signal and noise in the neural output. Theoretically, the assumption that neural systems maximize mutual information between salient features of the stimulus and neural output has allowed scientists to predict neural codes from signal processing models: for instance, the center-surround structure of human retinal neurons matches theoretical constructions for the optimal filter based on correlations found in natural images [cite].

The mutual information measures the information "capacity" of a channel consisting of an input $\boldsymbol{X}$ and an output $\boldsymbol{Y}$, and satisfies a number of important properties.

1. The channel input $\boldsymbol{X}$ and output $\boldsymbol{Y}$ can be random vectors of arbitrary dimension, and the mutual information remains a scalar functional of the joint distribution P of $(\boldsymbol{X}, \boldsymbol{Y})$.

2. When $\boldsymbol{X}$ and $\boldsymbol{Y}$ are independent, $\mathrm{I}(\boldsymbol{X}; \boldsymbol{Y}) = 0$; otherwise, $\mathrm{I}(\boldsymbol{X}; \boldsymbol{Y}) > 0$.

3. The data-processing inequality: for any vector-valued function $\vec{f}$ of the output space,
$$\mathrm{I}(\boldsymbol{X}; \vec{f}(\boldsymbol{Y})) \leq \mathrm{I}(\boldsymbol{X}; \boldsymbol{Y}).$$

4. Symmetry: $\mathrm{I}(\boldsymbol{X}; \boldsymbol{Y}) = \mathrm{I}(\boldsymbol{Y}; \boldsymbol{X})$.

5. Independent additivity: if $(\boldsymbol{X}_1, \boldsymbol{Y}_1)$ is independent of $(\boldsymbol{X}_2, \boldsymbol{Y}_2)$, then
$$\mathrm{I}((\boldsymbol{X}_1, \boldsymbol{Y}_1); (\boldsymbol{X}_2, \boldsymbol{Y}_2)) = \mathrm{I}(\boldsymbol{X}_1; \boldsymbol{Y}_1) + \mathrm{I}(\boldsymbol{X}_2; \boldsymbol{Y}_2).$$

Three additional consequences result from the data-processing inequality:

---

[2]Note that the mutual information is invariant with respect to change-of-measure.

- *Stochastic data-processing inequality* If $\vec{f}$ is a stochastic function independent of both $\boldsymbol{X}$ and $\boldsymbol{Y}$, then

$$\mathrm{I}(\boldsymbol{X}; \vec{f}(\boldsymbol{Y})) \leq \mathrm{I}(\boldsymbol{X}; \boldsymbol{Y}).$$

  This can be shown as follows: any stochastic function $\vec{f}(\boldsymbol{Y})$ can be expressed as a deterministic function $\vec{g}(\boldsymbol{Y}, W)$, where W is a random variable independent of $\boldsymbol{X}$ and $\boldsymbol{Y}$. By independent additivity,

$$\mathrm{I}(\boldsymbol{X}; \boldsymbol{Y}) = \mathrm{I}(\boldsymbol{X}; (\boldsymbol{Y}, W)).$$

  Then, by the data-processing inequality,

$$\mathrm{I}(\boldsymbol{X}; \boldsymbol{Y}) = \mathrm{I}(\boldsymbol{X}; (\boldsymbol{Y}, W)) \geq \mathrm{I}(\boldsymbol{X}; \vec{g}(\boldsymbol{Y}, W)) = \mathrm{I}(\boldsymbol{X}; \vec{f}(\boldsymbol{Y})).$$

- *Invariance under bijections.* If $\vec{f}$ has an inverse $\vec{f}^{-1}$, then

$$\mathrm{I}(\boldsymbol{X}; \vec{f}(\boldsymbol{Y})) \leq \mathrm{I}(\boldsymbol{X}; \boldsymbol{Y}) = \mathrm{I}(\boldsymbol{X}; \vec{f}^{-1}(\vec{f}(\boldsymbol{Y}))) \leq \mathrm{I}(\boldsymbol{X}; \vec{f}(\boldsymbol{Y})),$$

  therefore, $\mathrm{I}(\boldsymbol{X}; \vec{f}(\boldsymbol{Y})) = \mathrm{I}(\boldsymbol{X}; \boldsymbol{Y})$.

- *Monotonicity with respect to inclusion of outputs.* Suppose we have an output ensemble $(\boldsymbol{Y}_1, \boldsymbol{Y}_2)$. Then the individual component $\boldsymbol{Y}_1$ can be obtained as a projection of the ensemble. By the data-processing inequality, we therefore have

$$\mathrm{I}(\boldsymbol{X}; \boldsymbol{Y}_1) \leq \mathrm{I}(\boldsymbol{X}; (\boldsymbol{Y}_1, \boldsymbol{Y}_2)).$$

  Intuitively, if we observe both $\boldsymbol{Y}_1$ and $\boldsymbol{Y}_2$, this can only *increase* the information we have about $\boldsymbol{X}$ compared to the case where we only observe $\boldsymbol{Y}_1$ by itself.

And it is the property of *invariance under bijections*, inclusive of non-linear bijections, which qualifies mutual information as a *non-linear measure of dependence.* Linear correlations are invariant under scaling and translation, but not invariant to *nonlinear* bijections.

Besides the formal definition, there are a number of well-known alternative characterizations of mutual information in terms of other information-theoretic quantities: the *entropy* H:

$$\mathrm{H}_\mu(\boldsymbol{X}) = -\int p(\boldsymbol{X}) \log p(\boldsymbol{X}) d\mu(\boldsymbol{X}),$$

and the *conditional entropy*:

$$\mathrm{H}_\mu(\boldsymbol{X}|\boldsymbol{Y}) = -\int p(\boldsymbol{Y}) d\mu_y(\boldsymbol{Y}) \int p(\boldsymbol{X}|\boldsymbol{Y}) \log p(\boldsymbol{X}|\boldsymbol{Y}) d\mu_x(\boldsymbol{X}).$$

Some care needs to be taken with entropy and conditional entropy since they are not invariant with respect to change-of-measure: hence the use of the subscript in the notation H_μ. In particular, there is a difference between *discrete entropy* (when μ is the counting measure) and *differential entropy* (when μ is p-dimensional Lesbegue measure.) Intuitively, entropy measures an observer's uncertainty of the random variable $\boldsymbol{X}$, supposing the observer has no prior information other than the distribution of $\boldsymbol{X}$. Conditional entropy measures the *expected uncertainty* of $\boldsymbol{X}$ supposing the observer observes $\boldsymbol{Y}$.

The following identities characterize mutual information in terms of entropy:

$$\mathrm{I}(\boldsymbol{X}; \boldsymbol{Y}) = \mathrm{H}_{\mu_x \times \mu_y}((\boldsymbol{X}, \boldsymbol{Y})) - \mathrm{H}_{\mu_x}(\boldsymbol{X}) - \mathrm{H}_{\mu_y}(\boldsymbol{Y}).$$

$$\mathrm{I}(\boldsymbol{X};\boldsymbol{Y}) = \mathrm{H}_\mu(\boldsymbol{Y}) - \mathrm{H}_\mu(\boldsymbol{Y}|\boldsymbol{X}). \tag{1.1}$$

The second identity (1.1) is noteworthy as being practically important for estimation of mutual information. Since the entropies in question only depend on the marginal and conditional distributions of $\boldsymbol{Y}$, the problem of estimating $\mathrm{I}(\boldsymbol{X};\boldsymbol{Y})$ can be reduced from a $\dim(\boldsymbol{X}) + \dim(\boldsymbol{Y})$-dimensional nonparametric estimation problem to a $\dim(\boldsymbol{Y})$-dimensional problem: hence this identity is a basis of several methods of estimation used in neuroscience, such as Gastpar (2014).

However, by symmetry, we also have the flipped identity

$$\mathrm{I}(\boldsymbol{X};\boldsymbol{Y}) = \mathrm{H}_\mu(\boldsymbol{X}) - \mathrm{H}_\mu(\boldsymbol{X}|\boldsymbol{Y}). \tag{1.2}$$

In neuroscience studies, where $\boldsymbol{X}$ is the controlled stimulus, and $\boldsymbol{Y}$ is the neural activity, the two mirror pairs (1.1) and (1.2) have different interpretations. Rather than providing a basis for practical estimation, (1.2) provides an *interpretation* of the mutual information. Loosely speaking, $\mathrm{H}_\mu(\boldsymbol{X})$ is the uncertainty of $\boldsymbol{X}$ before having observed $\boldsymbol{Y}$, and $\mathrm{H}_\mu(\boldsymbol{X}|\boldsymbol{Y})$ is the uncertainty of $\boldsymbol{X}$ after having observed $\boldsymbol{Y}$, hence $\mathrm{H}_\mu(\boldsymbol{X}) - \mathrm{H}_\mu(\boldsymbol{X}|\boldsymbol{Y})$ is how much the observation of $\boldsymbol{Y}$ has *reduced* the uncertainty of $\boldsymbol{X}$. Stated in words,

$$\mathrm{I}(\boldsymbol{X};\boldsymbol{Y}) = \text{average reduction of uncertainty about } \boldsymbol{X} \text{ upon observing } \boldsymbol{Y}.$$

1.2.3   Comparisons

Therefore, we see that in both the multi-class classification problem and the noisy channel model present examples of discrimination problems where one must recover some latent variable Y from observations X, where X is related to Y through the family of conditional distributions $F_{X|Y}$. One difference is that while in multi-class classification, $F_{X|Y}$ is unknown and has to be inferred from data, in the noisy channel model, the stochastic properties of the channel $F_{X|Y}$ are usually assumed to be known. For example, for a binary channel where Y consists of an m-length binary string, a commonly studied channel $F_{X|Y}$ generates X by randomly flipping bits in Y independently with some probability ϵ. A second difference is that in the noisy channel model, there is a choice in how to specify the encoding function $g(M)$, which affects subsequent performance. Finally, in the broader research context, machine learning research has traditionally focused on multi-class problems with relatively few classes, while information theory tends to consider problems in asymptotic regimes where the number of possible messages m is taken to infinity. These differences were sufficient to explain why little overlap exists in the respective literatures between multi-class classification and the noisy channel model.

However, an interesting development in the machine learning community has been the application of multi-class classification to problems with increasingly large and complex label sets. Consider the following timeline of representative papers in the multi-class classification literature:

- Fisher's Iris data set, Fisher 1936, $K = 3$ classes

- Letter recognition, Frey and Slate 1991, $K = 26$ classes

- Michalski's soybean dataset, Mickalstd 1980, $K = 15$ classes

- The NIST handwritten digits data set, Grother 1995, $K = 10$ classes

- Phoneme recognition on the TIMIT datset, Clarkson and Moreno 1999, $K = 39$ classes

- Object categorization using Corel images, Duygulu et al. 2002 $K = 371$ classes

- Object categorization for ImageNet dataset, Deng et al. 2010, $K = 10,184$ classes

- The 2nd Kaggle large-scale hierarchical text classification challenge (LSHTC), Partalas et al. 2015, $K = 325,056$

As we can see, in recent times we begin to see classification problems with extremely large label sets. In such large-scale classification problems, or 'extreme' classification problems, results for $K \to \infty$ numbers of classes, like those found in information theory, begin to look more applicable.

This work focuses on a particular intersection between multi-class classification and information theory, which is the study of *random classification tasks.* In numerous domains of applied mathematics, it has been found that systems with large numbers of components can be modelled using randomized versions of those same systems, which are more tractable to mathematical analysis: for example, studying the properties of networks by studying random graphs in graph theory, or studying the performance of combinatorial optimization algorithms for random problem instances. Similarly, it makes sense to posit randomized models of multi-class discrimination problems. Since information theorists were the first to study discrimination problems with large number of classes, we find in the information theory literature a long tradition of the study of *random code* models, dating back all the way to Shannon's seminal 1948 paper. This thesis is dedicated to the the study of the analogue of random code models in the multi-class classification setting: models of *randomized classification.*

1.3 Applications of supervised learning and information theory in neuroscience

The study of naturally intelligent systems, and the study and design of artificially intelligent systems, form two major intertwining domains of modern research. Here, we take *intelligence* to refer to the property of a system by which it can modulate its reaction to external inputs in a purposeful manner. Therefore, by this definition, an amoeba which seeks food and avoids toxins is intelligent, as is a gene-regulation network, or a mammalian brain. Similarly, artificially intelligent algorithms which implement automated decision-making rules in response to external inputs also satisfy this definition of intelligence.

A primitive organism may classify percieved objects in its environment as either beneficial (potential food and resources) or harmful (toxins and predators), and intelligently respond by means of pursuing the former and avoiding the latter. Complex organisms, like humans, not only discriminate in order to make immediate decisions, but also categorize objects in the world in order to perform intermediate calculations and carry out contextual reasoning.

Similarly, *artificially intelligent* algorithms and agents will also discriminate input data into categories. Very often, these types of classification and recognition tasks mimic and automate discrimination tasks that humans already perform, such as:

- Optical character recognition: recognizing characters from handwritten glyphs.

- Facial recognition: identifying individuals from images of their faces.

- Object recognition: identifying objects in photographs and labelling them with the appropriate keyword.

However, classification can also be performed on novel types of tasks where no human substitute exists, such as diagnosis of cancer phenotype based on thousands of gene expression levels.

While a major use of artificially intelligent classifiers is to automate routine tasks or to categorize complex data, it is also scientifically interesting to compare the performance of naturally intelligent agents (human or animal subjects) versus artificially intelligent classifiers on discrimination tasks. One reason is that human benchmarks on complex classification tasks, such as object recognition, are often non-trivial to beat, and provide a useful reference to quantify progress in machine learning. Yet, another reason is that the attempt to engineer an artificially intelligent solution to a natural recognition problem provides insight into the nature of intelligence in human and animal brains. We still cannot fully explain the human capability to quickly locate and identify objects in a natural scene, but research into the mechanisms of vision, and attempts to replicate human capabilities for object recognition, have already provided crucial insight into the hierarchical nature of mammalian vision.

The approach of using classifiers as models of cognition is especially valuable for the problem of understanding specialization in the brain. Historically, the earliest discoveries of specialized modules in the brain were due to lesion studies, where patients who had parts of their brain destroyed due to injury or clinical surgeries also lost cognitive or motor functionality as a result. The loss of functionality established a causal pathway between the lesioned area and the affected behavior–as, for example, in the case of the discovery of Broca's area, which was established in this way to be critical for speech production [CITE]. However, ethical and practical limitations restrict the use of lesioning as an experimental technique, and furthermore, lesion studies cannot be applied to exhaustively isolate the regions of the brain which are specialized for a given task. Therefore, an alternative method of studying specialization is to acquire an image of the brain activity, and then to assess the discriminative performance of classifiers on either the whole brain, the brain minus a number of "lesioned" areas, or isolated regions of the brain by themselves. The classifier may achieve a certain accuracy using the whole brain image, and reduced accuracies using "lesioned" images–and, given the removal of the task-critical parts of the brain in the image, may be reduced to chance accuracy levels. Therefore, similar to lesion studies, these classification experiments can reveal specialization in the brain by establishing which parts of the brain image contain *information* related to the task. However, an important distinction is that these studies can only establish association, rather than causality, because actual lesions to the brain affect the activity patterns of other parts of the brain, and therefore the effect of lesions cannot actually be completely simulated by merely masking parts of the brain image.

However, a potentially puzzling aspect of this approach, is that the structure or dynamics of the artificially intelligent classifier need not imitate the dynamics of the biological system for the modelling approach to be useful. Computational neuroscientists have developed biological realistic models of neural signalling activity which could be employed to simulate the neural decision-making process from input to output, at a very high level of versimilitude. However, it is often more useful in practice to model the decision-making process with much simpler statistical models, such as linear regression. Even relatively complex machine learning models, such as deep neural networks, represent a vast simplification from biological dynamics.

Yet their use can often be justified by the assumption that the performance achieved on this task by the given classifier is reflective of the performance that would be achieved by a more biologically realistic model. Indeed, this assumption can often be justified because, as is generally observed in real-world machine learning applications, several very different types of classifiers often end up achieving similar performance (when tuned correctly).

How can we explain the correlation in the performance of very different families of classifiers across problems in a wide range of domains? In problems where it is hard to a given family of classifiers to perform well, it is also hard to other families of classifiers. In problems where one classifier achieves very high accuracy, many other families of classifier can achieve high accuracy as well.

One explanation for this phenomenon is that the input contains a certain amount of *information* about the output, and that the amount of information sets fundamental limits on what kind of classification accuracies can be achieved. Indeed, the relationship between information and bounds on discrimination accuracy were first established by Claude Shannon, who gave the formula for the *mutual information* between two random variables X and Y, and whose proved in his noisy-channel theorem an asymptotic relationship between the mutual information and achievable discrimination accuracy. Fano [CITE] followed this result with the equally classical Fano's inequality, which establishes an upper bound on accuracy as a function of mutual information.

Neuroscientists have used the connection between information and discrimination in several ways. One is to sidestep the application of classifiers altogether, and to directly estimate the mutual information between brain activity and the task of interest [CITE]. A second way to to proceed with training classifiers on the data, but then summarizing the performance of the classifier by the mutual information implied by the confusion matrix. Hence, implied mutual information becomes a error metric for the classification–but one that is more readily comparable across different classification tasks.

[OK, now what do we do? We play around with the connection between MI and discrimination some more, and find some things.]

We list these properties of mutual information in preparation for section **??**, where we prepare a "minimal" set of properties for an information coefficient, and consider how much of the functionality of the mutual information would be preserved by an alternative information coefficient satisfying only those minimal properties.

But what, exactly, is the functionality of mutual information in neuroscience? How it is used in practice? A nice summary of the applications of mutual information is provided in the introduction of Gastpar (2014). Taking their list as a starting point, we briefly overview the main use-cases of mutual information, and illustrate each with a representative example.

Selecting decoding models.

Neurons carry information via *spike trains*, which are temporal point processes. In response to stimulus $\boldsymbol{X}$, the neuron produces a spike train $Y(t)$ where $Y(t) = 1$ indicates a spike at time t and $Y(t) = 0$ indicates no spiking, for $t \in [0, T]$.

An open question in neuroscience that of how information is encoded in the spike train. Put loosely, what is 'signal' in the spike train $Y(t)$ and what is 'noise'? Presumably there exists some *decoder*–some function $\vec{g}$ of the time series, which compresses $Y(t)$ to a small dimension while preserving most of the information about $\boldsymbol{X}$.

Nelken et. al. (2005) investigated the neural code in the A1 auditory cortex of a cat, in response to recorded birdsongs. The stimulus $\boldsymbol{X} = (X_1, X_2)$ takes the form of 15 different auditory recordings presented in 24 spatial directions: $X_1 \in \{1, \dots, 15\}$ indexes the recording and $X_2 \in \{1, \dots, 24\}$ indexes the direction of presentation. The response $Y(t)$ takes the form of a spike train.

Nelkin et. al. compare the following *decoders* $\vec{g}$ in terms of the information $\mathrm{I}(\boldsymbol{X}; \vec{g}(Y(t)))$.

- The total spike count $\vec{g}_1(Y(t)) = \sum_t Y(t)$.

- The mean response time $\vec{g}_2(Y(t)) = \frac{1}{\sum_t Y(t)} \sum_t t Y(t)$.

- The combination of the two codes: $\vec{g}_{1+2}(Y(t)) = (\vec{g}_1(Y(t)), \vec{g}_2(Y(t)))$.

The information of each decoder is compared to the full information of the signal, $\mathrm{I}(\boldsymbol{X}; Y(t))$, which is estimated via binning.

Nelkin et al. find that while the decoder $\vec{g}_1$ reduces the mutual information by 20 to 90 percent, the information loss from $\vec{g}_2$ is much less, and barely any information at all is lost when both decoders are used jointly in $\vec{g}_{1+2}$. The scientific conclusion that can be drawn is that since $\mathrm{I}(\boldsymbol{X}; \vec{g}_{1+2}(Y(t)))$ is not much smaller than $\mathrm{I}(\boldsymbol{X}; Y(t))$, the "signal" in the spike train is mostly captured by the spike counts and response times: beyond that, the detailed temporal pattern of spiking is likely to be "noise." Of course, an important caveat to their conclusions is only *individual* neurons are considered: the analysis did not rule out the possibility that the temporal spiking pattern could yield information within an *ensemble* of neurons.

- Example: Redundancy in population code of retina. Property (i)-(iii) and (v) are needed to obtain a meaningful measure of redundancy.

- In general, symmetry not important, but additivity is desirable for measures of redundancy. Property (ii) can usually be enforced since any measure needs to have a unique "minimum" value for the case of independence.

1.4   Random codes and random classification

A random code model in information theory is one where given some distribution ν (typically a uniform distribution) on the space of transmittable signals $\mathcal{Y}$, we posit that the decoder $g(M)$ is randomly generated, by letting $g(1), \dots, g(m)$ be identically and independently assigned to random draws from ν. For example, when $\mathcal{Y}$ is the space of m-length binary strings, the encoder g maps indices $1, \dots, m$ to random m-length binary strings. The purpose of the random code model is usually to establish a lower bound on achievable accuracy given some constraints on the signal space.

Meanwhile, a randomized classification model is one where the label set $\{y^{(1)}, \dots, y^{(k)}\}$ is not fixed, but randomly sampled. One defines a label space $\mathcal{Y}$, a family of conditional distributions $\{F_{X|y}\}_{y \in \mathcal{Y}}$, and a distribution ν on $\mathcal{Y}$. Then the randomized classification model is a classification task obtained by drawing labels $\{Y^{(1)}, \dots, Y^{(k)}\}$ iid from ν, generating training data for those particular labels by drawing observations $X_i^{(j)} \sim F_{X|Y^{(j)}}$, and where the problem is to construct a classification rule for assigning new observations X which are drawn from the mixture

$$X \sim \frac{1}{k} \sum_{i=1}^{k} F_{X|Y^{(k)}}$$

to one of the labels $\{Y^{(1)}, \ldots, Y^{(k)}\}$. As we will see throughout the thesis, the randomized classification model can be naturally applied to a large number of multiclass classification applications, such as facial recognition, where the labels (e.g. people) can be justifiably modelled as random draws from some population. And, even in the majority of classification problems where the labels cannot be assumed to come from an iid sample, randomized classification models can still be applied to provide intuition for the original problem.

The link between random code models and randomized classification models should now be apparent. Define $Y_i = g(i)$ in the random code model, so that Y_i are iid drawn from ν. Fixing a particular realization of $Y_1, \ldots, Y_k$, the decoding problem is then evidently a multi-class classification problem with labels $\{Y_1, \ldots, Y_k\}$. The only difference between the two models is that the conditional distributions $F_{X|Y}$ are assumed to be known in the random code model, and assumed unknown in the randomized classification model.

But happens when we assume that $F_{X|Y}$ is known, in the multi-class classification problem? In fact, it is common to consider the case of known $F_{X|Y}$ in the machine learning literature, because the resulting accruacy gives an *upper bound* on achievable performance in the multi-class classification problem. This is because once $F_{X|Y}$ is known, it is possible to define the *optimal* classification rule, or *Bayes* classification rule h_{Bayes}. For example, supposing that the performance criterion is to minimize the zero-one risk $\Pr[\hat{Y} \neq Y]$, then the Bayes rule is to assign X to the label with the highest posterior density,

$$h_{Bayes}(X) = \text{argmax}_{y \in \{y_1, \ldots, y_k\}} f_{X|y}(x)\pi(y)$$

where $\pi(y)$ is the prior probability of $Y = y$. Therefore, it is the same thing to study the Bayes accuracy in a randomized classification model and the decoding accuracy of a randomized code in a noisy channel.

Indeed, the analysis of the Bayes accuracy of a randomized classification model forms the subject of Chapters 2 and 3. Due to the aforementioned equivalence, it can be said that a large body of work dealing with the Bayes accuracy of randomized classification problems exists in information theory: however, the majority of such works deal with the limit as $k \to \infty$, and to our knowledge no analysis has been done for the case of finite k, which is the relevant scenario for multi-class classification. There is good reason for this lacuna in the information theory literature, which is that since information theorists are concerned with understanding the properties of *optimal* coding schemes, it follows that randomized coding schemes are only interesting insofar as that they give good approximations to optimal coding schemes. However, in the classification setting, we may be interested in studying randomized classification for its own sake, and not merely as a means to obtain lower bounds or estimates for another problem. Therefore, Chapter 2 presents novel results on the statistical properties of the Bayes accuracy in the randomized classification model. Meanwhile, Chapter 3 studies an interesting application of the randomized classification problem, which is to analyze the dependence of the classification accuracy on the size of the label set. This analysis yields a novel method for 'performance extrapolation' in real-world classification problems, meaning that our method can be used to estimate the classification accuracy on a large multi-class classification problem using data from only a subsample of the classes in the larger problem.

Chapter 2

Randomized classification

2.1 Motivation

2.1.1 Facial recognition example

2.2 Setup

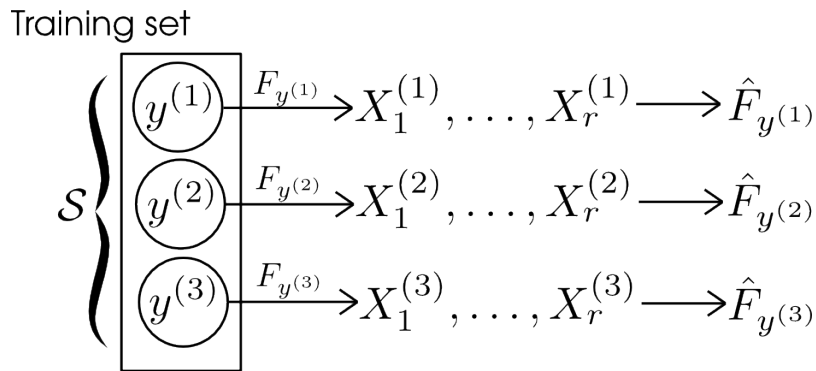### 2.2.1 Sampling scheme

Training set

FIGURE 2.1: Training set

A *classification task* consists of a subset of labels, $\mathcal{S} \subset \mathcal{Y}$. Write $\mathcal{S} = \{y_1, \ldots, y_k\}$, where k is the number of classes. It is convenient to decouple the joint distribution of (X, Y) into a prior distribution over the k labels $\mathcal{S}_k$, and the conditional distribution of elements, or feature vectors describing them, within a label class $X|Y = y \sim F_y$.

We would like to identify the sources of randomness in evaluating a classifier. First, there is the specific choice of k classes for the label set. Second, there is randomness in training the classifier for these classes, which comes from the use of a finite training set. Third, there is the randomness in the observed accuracy when testing the classifier on a test set. In order to separate these three sources, we need to clarify some terms used ambiguously in the classification literature.

We call a *classification rule* a function f which maps feature vectors $x \in \mathcal{X}$ to the set of labels $\mathcal{S}$:

$$f : \mathcal{X} \to \mathcal{S}.$$

For a random class Y drawn according to the uniform distribution[1] on $\mathcal{S}$ and a feature vector drawn under F_Y, the loss of $\ell(f(X), Y)$ is obtained. The *risk*, or expected

---

[1]See the discussion for extensions to non-uniform priors.

Classification Rule

$$M_{y^{(1)}}(x) = \mathcal{M}(\hat{F}_{y^{(1)}})(x)$$

$$M_{y^{(2)}}(x) = \mathcal{M}(\hat{F}_{y^{(2)}})(x)$$

$$M_{y^{(3)}}(x) = \mathcal{M}(\hat{F}_{y^{(3)}})(x)$$

$$\hat{Y}(x) = \operatorname{argmax}_{y \in \mathcal{S}} M_y(x)$$
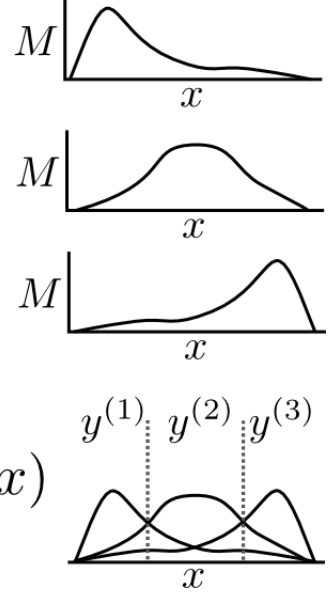
FIGURE 2.2: Classification rule

loss, of the classification rule is

$$\text{Risk}(f; \pi, \ell) = \int \ell(f(X), Y) dF_Y d\pi.$$

For now, we will assume a 0–1 loss and a uniform prior over the labels in $\mathcal{S}$. Therefore, the risk can be rewritten as

$$\text{Risk}(f; \mathcal{S}, \ell_{01}) = \frac{1}{k} \sum_{y_i \in \mathcal{S}} \Pr(f(X) \neq y_i; X \sim F_{y_i}).$$

The classification rule itself can be seen as a random function that depends on the sampling of the training set. For convenience, assume that the training set is composed of r i.i.d examples for each label $y \in \mathcal{S}$ (a total of $k \times r$). An i.i.d. sample of size r, $X_1, \ldots, X_r \sim F_y$ can also be described as an empirical distribution, using the shorthand $\hat{F}_y$.

$$\hat{F}_y = \frac{1}{r} \sum_{i=1}^{r} \delta_{x_i^{(y)}}.$$

A *classifier* $\mathcal{F}$ is the algorithm or procedure for producing classification rules given a vector of empirical distributions $(\hat{F}_y)_{y \in \mathcal{S}}$. The classifier maps the empirical distributions to a classification rule f (Figure 2.2).

We can therefore describe the r-repeat risk of the model $\mathcal{F}$ as the expected risk of a classification rule $\hat{f}$ trained using a sample of size r from each of labels in $\mathcal{S}_k$.

That is,

$$\text{Risk}_r(\mathcal{F}; \pi) = \int \text{Risk}(\mathcal{F}(\{\hat{F}_y\}_{y \in \mathcal{S}}; \mathcal{S}, \ell) \prod_{y \in \mathcal{S}} d\Pi_{y,r}(\hat{F}_y).$$

Figure 2.3 illustrates the variables involved in defining the risk.
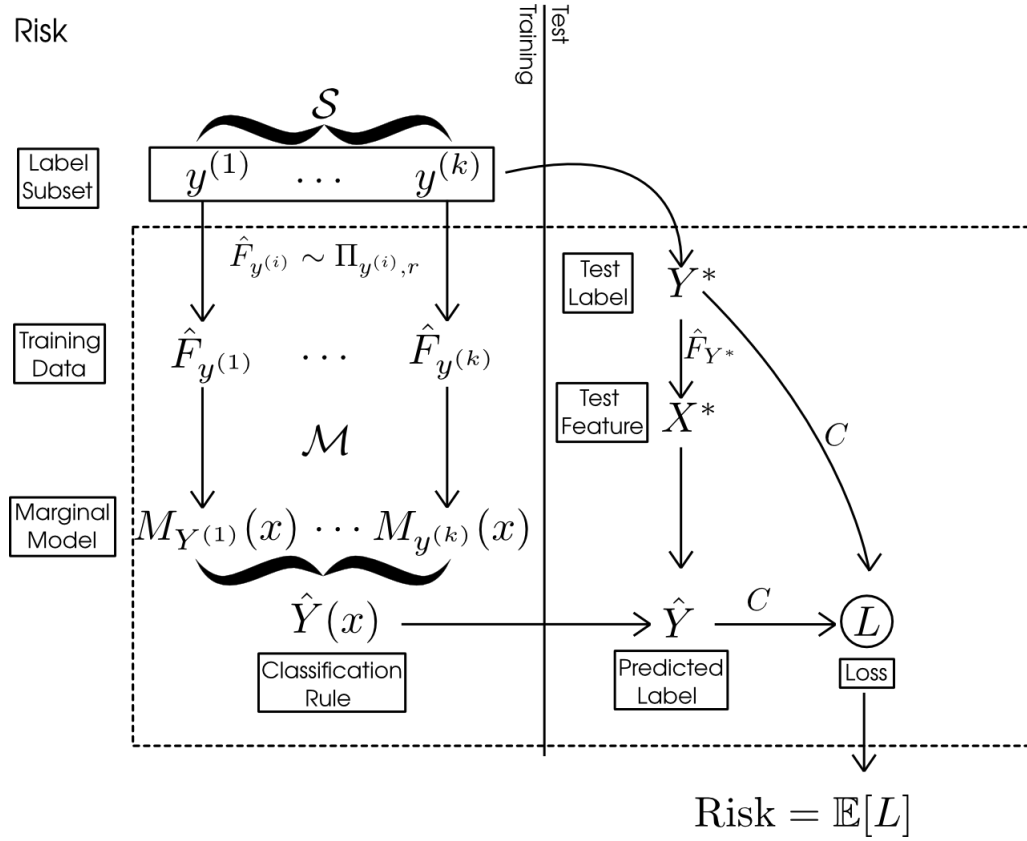
FIGURE 2.3: Classification risk

2.2.2 Average accuracy

Since the classification tasks are randomly generated, the r-repeat risk becomes a *random variable* which depends on the random label subset $\mathcal{S}$.

Therefore, define the k-class, r-repeat *average risk* of classifier $\mathcal{F}$ as

$$\text{AvRisk}_{k,r}(\mathcal{F}) = \mathbf{E}[\text{Risk}_k(\mathcal{F})]$$

where the expectation is taken over the distribution of $\mathcal{S} = (Y^{(1)}, \ldots, Y^{(k)})$ when $Y^{(i)} \overset{iid}{\sim} \text{Unif}(\mathcal{S})$.

As we can see from Figure 2.4, the average risk is obtained by averaging over four randomizations:

A1. Drawing the label subset $\mathcal{S}$.

A2. Drawing the training dataset.

A3. Drawing Y^* uniformly at random from $\mathcal{S}$.

A4. Drawing X^* from F_{X^*}.

For the sake of developing a better intuition of the average risk, it is helpful to define a random variable called the *loss*, which is the cost incurred by a single test instance. The loss is determined by quantities from all four randomization steps: the label subset $\mathcal{S} = \{Y^{(1)}, \ldots, Y^{(k)}\}$, the training samples $\hat{F}_{Y^{(1)}}, \ldots, \hat{F}_{Y^{(k)}}$, and the test point (X^*, Y^*). Formally, we write

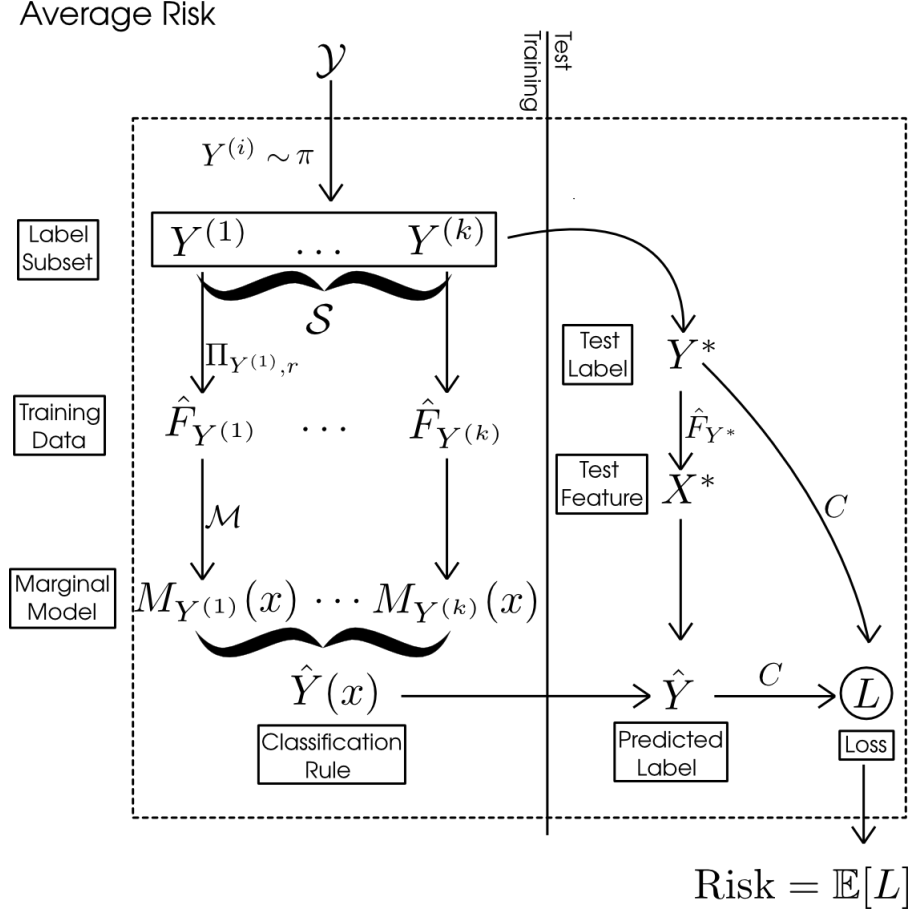$$L = C(\mathcal{F}(\{\hat{F}_y\}_{y \in \mathcal{S}})(X^*), Y^*).$$

FIGURE 2.4: Average risk

Now note that the k-class, r-repeat average risk is the expected loss,

$$\text{AvRisk}_{k,r,\nu}(\mathcal{F}) = \mathbf{E}[L] = \mathbf{E}[C(\mathcal{F}(\{\hat{F}_y\}_{y \in \mathcal{S}})(X^*), Y^*)]. \tag{2.1}$$

where the expectation is taken over the joint distribution of all the quantities $\{Y^{(1)}, \ldots, Y^{(k)}, \hat{F}_{Y^{(1)}}, \ldots,$

We will aim to develop a method for estimating the *average risk*. In the case where the classification tasks are independently generated, the average risk is the best predictor (in mean-squared error) for the (random) risk.

2.3 Estimation of average accuracy

2.3.1 Subsampling method

In the special case where $k_1 = k_2 = k$: that is, where the label subsets $\mathcal{S}_1$ and $\mathcal{S}_2$ are the same size, it is clear to see that any unbiased estimate of the risk of the classifier $\mathcal{F}$ for the first classification problem is an unbiased estimate of the average k-class risk. The *test risk* gives one such unbiased estimate of the average k-class risk.

Recall that the data consists of class labels $y^{(i)}$ for $i = 1, \ldots, k_1$, as well as training sample $\hat{F}_{y^{(i)}}$ and test sample $(x_1^{(i)}, \ldots, x_{r_{test}}^{(i)})$ for $i = 1, \ldots, k_1$.

For any given test observation $x_j^{(i)}$, we obtain the predicted label $\hat{y}_j^{(i)}$ by computing the margin for each class,

$$M_{i,j,\ell} = \mathcal{M}(\hat{F}_{y^{(\ell)}})(x_j^{(i)}) = m_{y^{(\ell)}}(x_i^{(j)}),$$

for $\ell = 1, \ldots, k$, and by finding the class with the highest margin $M_{i,j,\ell}$,

$$\hat{y}_j^{(i)} = y_{\mathrm{argmax}_\ell M_{i,j,\ell}}.$$

The test risk is the average cost over test observations,

$$\text{Test Risk} = \frac{1}{r_{test}k} \sum_{i=1}^{k} \sum_{j=1}^{r_{test}} C(\hat{y}_j^{(i)}, y^{(i)}). \tag{2.2}$$

For each test observation, define the ranks of the margins by

$$R_{i,j,\ell} = \sum_{m \neq \ell} I\{M_{i,j,\ell} \geq M_{i,j,m}\}.$$

Therefore, $\hat{y}_j^{(i)}$ is equal to ℓ if and only if $R_{i,j,\ell} = k$. Thus, an equivalent expression for test risk is

$$\text{Test Risk} = \frac{1}{r_{test}k} \sum_{i=1}^{k} \sum_{\ell=1}^{k} \sum_{j=1}^{r_{test}} C_{ij} I\{R_{ij\ell} = k\}. \tag{2.3}$$

where

$$C_{ij} = C(y^{(j)}, y^{(i)}).$$

Besides the test risk, other methods, such as cross-validation, can also be used to obtain estimates of the average k-class risk.

Suppose we have data for k_1 classes, and we wish to estimate AvRisk_{k_2} for $k_2 \leq k_1$. Let $\mathcal{S}_1 = \{y_1, \ldots, y_{k_1}\}$. To obtain a classification problem with k_2 classes, we can simply pick a subset S of size k_2 from $\mathcal{S}_1$, and throw away all the training and test data from the other classes $\mathcal{S} \setminus S$. Then, the test risk (2.3) gives an unbiased estimate of the AvRisk_{k_2}.

Of course, one could obtain a better estimator of the average risk by averaging over all the subsets $S \subset \mathcal{S}_1$ of size k_2. For general classifiers, this may require retraining a classifier over each subset. However, for marginal classifiers, one can compute the average test risk over all $\binom{k_1}{k_2}$ subsets easily.

The reason why the efficient computation is possible is because the test risk for each subproblem can be determined by looking at the margins $M_{i,j,\ell}$, which remain the same as long as both i and ℓ are included in the subsample S.

The computational trick is to look at each combination of test observation $x_j^{(i)}$ and class label $y^{(\ell)}$, and to count the number of subsets $N_{i,j,\ell}$ where (i) both i and ℓ are included in S, and (ii) $\hat{y}_j^{(i)} = y^{(\ell)}$. Then it should be clear that the average test risk over all subsets is equal to

$$\text{AvTestRisk}_{k_2} = \frac{1}{\binom{k_1}{k_2}} \frac{1}{r_{test}k_2} \sum_{i=1}^{k_1} \sum_{\ell \neq i} \sum_{j=1}^{r_{test}} C_{i\ell} N_{i,j,\ell}. \tag{2.4}$$

Now it is just a matter of simple combinatorics to compute $N_{i,j,\ell}$. We require both $y^{(i)}$ and $y^{(\ell)}$ to be included in S. This implies that if $M_{i,j,i} > M_{i,j,\ell}$, then $y^{(\ell)}$ will

never have the highest margin in any of those subsets, so $N_{i,j,\ell} = 0$.

Otherwise, there are $R_{i,j,\ell} - 1$ elements in $\mathcal{S}_1$ with a lower margin than $y^{(\ell)}$. Since $i \neq \ell$, then there are $k_2 - 2$ elements in $S \setminus \{i, \ell\}$, so therefore $N_{i,j,\ell} = \binom{R_{i,j,\ell}-2}{k_2-2}$. Therefore, we can write

$$N_{i,j,\ell} = I\{R_{i,j,\ell} > R_{i,j,i}\} \binom{R_{i,j,\ell} - 2}{k_2 - 2} \tag{2.5}$$

Therefore, the challenging case is when $k_2 > k_1$: we want to predict the performance of the classification model in a setting with more labels than we currently see in the training set.

2.3.2 Extrapolation

2.4 Average Bayes accuracy

The generalization accuracy of any classification rule is upper-bounded by the accuracy of the optimal classification rule, or *Bayes rule.* That is, one can define the *Bayes accuracy* as

$$\text{BA} = \sup_f \text{GA}(f).$$

And due to Bayes' theorem, the optimal classification rule f^* which achieves the Bayes accuracy can be given explicitly: it is the maximum a posteriori (MAP) rule

$$f^*(y) = \text{argmax}_{i=1}^k \, p(y|x^{(i)}).$$

Of course, it is not possible to construct this rule in practice since the joint distribution is unknown. Instead, a reasonable approach is to try a variety of classifiers, producing rules $f_1, \ldots, f_m$, and taking the best generalization accuracy as an estimate of the Bayes accuracy.

2.4.1 Definitions

Suppose X and Y are continuous random variables (or vectors) which have a joint distribution with density $p(x, y)$. Let $p(x) = \int p(x, y)dy$ and $p(y) = \int p(x, y)dx$ denote the respective marginal distributions, and $p(y|x) = p(x, y)/p(x)$ denote the conditional distribution.

ABA_k, or k-class Average Bayes accuracy is defined as follows. Let $X_1, ..., X_K$ be iid from $p(x)$, and draw Z uniformly from $1, .., k$. Draw $Y \sim p(y|X_Z)$. Then, the average Bayes accuracy is defined as

$$\text{ABA}_k[p(x, y)] = \sup_f \Pr[f(X_1, ..., X_k, Y) = Z]$$

where the supremum is taken over all functions f. A function f which achieves the supremum is

$$f_{Bayes}(x_1, ..., x_k, y) = \text{argmax}_{z \in \{1,...,k\}} p(y|x_z),$$

where an arbitrary rule can be employed to break ties. Such a function f_{Bayes} is called a *Bayes classification rule.* It follows that ABA_k is given explicitly by

$$\text{ABA}_k = \frac{1}{k} \int \left[\prod_{i=1}^k p(x_i)dx_i \right] \int dy \max_i p(y|x_i),$$

as stated in the following theorem.

Theorem 2.4.1 *For a joint distribution $p(x, y)$, define*

$$ABA_k[p(x, y)] = \sup_f \Pr[f(x_1, ..., x_k, y) = Z]$$

where $X_1, ..., X_K$ are iid from $p(x)$, Z is uniform from $1, .., k$, and $Y \sim p(y|X_Z)$, and the supremum is taken over all functions $f : \mathcal{X}^k \times \mathcal{Y} \to \{1, ..., k\}$. Then,

$$ABA_k = \frac{1}{k} \int \left[\prod_{i=1}^k p(x_i) dx_i \right] \int dy \max_i p(y|x_i).$$

Proof. First, we claim that the supremum is attained by choosing

$$f(x_1, ..., x_k, y) = \operatorname{argmax}_{z \in \{1, ..., k\}} p(y|x_z).$$

To show this claim, write

$$\sup_f \Pr[f(X_1, ..., X_k, Y) = Z] = \sup_f \frac{1}{k} \int p_X(x_1) \ldots p_X(x_k) p(y|x_{f(x_1,...,x_k,y)}) dx_1 \ldots dx_k dy$$

We see that maximizing $\Pr[f(X_1, ..., X_k, Y) = Z]$ over functions f additively decomposes into infinitely many subproblems, where in each subproblem we are given $\{x_1, ..., x_k, y\} \in \mathcal{X}^k \times \mathcal{Y}$, and our goal is to choose $f(x_1, ..., x_k, y)$ from the set $\{1, ..., k\}$ in order to maximize the quantity $p(y|x_{f(x_1,...,x_k,y)})$. In each subproblem, the maximum is attained by setting $f(x_1, ..., x_k, y) = \operatorname{argmax}_z p(y|x_z)$–and the resulting function f attains the supremum to the functional optimization problem. This proves the claim.

We therefore have

$$p(y|x_{f(x_1,...,x_k,y)}) = \max_{i=1}^k p(y|x_i).$$

Therefore, we can write

$$\begin{aligned}
ABA_k[p(x, y)] &= \sup_f \Pr[f(X_1, ..., X_k, Y) = Z] \\
&= \frac{1}{k} \int p_X(x_1) \ldots p_X(x_k) p(y|x_{f(x_1,...,x_k,y)}) dx_1 \ldots dx_k dy. \\
&= \frac{1}{k} \int p_X(x_1) \ldots p_X(x_k) \max_{i=1}^k p(y|x_i) dx_1 \ldots dx_k dy.
\end{aligned}$$

2.5 Variability of Bayes Accuracy

We have

$$ABA_k = \mathbf{E}[BA(X_1, ..., X_k)]$$

where the expectation is over the independent sampling of $X_1, ..., X_k$ from $p(x)$.

Therefore, $BA_k = BA(X_1, ..., X_k)$ is already an unbiased estimator of ABA_k. However, to get confidence intervals for ABA_k, we also need to know the variability.

We have the following upper bound on the variability.

Theorem 2.5.1 *Given joint density $p(x, y)$, for $X_1, ..., X_k \overset{iid}{\sim} p(x)$, we have*

$$Var[BA(X_1, ..., X_k)] \le \frac{1}{4k}.$$

Proof. According to the Efron-Stein lemma,

$$\text{Var}[\text{BA}(X_1, ..., X_k)] \leq \sum_{i=1}^{k} \mathbf{E}[\text{Var}[\text{BA}|X_1, ..., X_{i-1}, X_{i+1}, ..., X_k]].$$

which is the same as

$$\text{Var}[\text{BA}(X_1, ..., X_k)] \leq k\mathbf{E}[\text{Var}[\text{BA}|X_1, ..., X_{k-1}]].$$

The term $\text{Var}[\text{BA}|X_1, ..., X_{k-1}]$ is the variance of $\text{BA}(X_1, ..., X_k)$ conditional on fixing the first $k-1$ curves $p(y|x_1), ..., p(y|x_{k-1})$ and allowing the final curve $p(y|X_k)$ to vary randomly.

Note the following trivial results

$$-p(y|x_k) + \max_{i=1}^{k} p(y|x_i) \leq \max_{i=1}^{k-1} p(y|x_i) \leq \max_{i=1}^{k} p(y|x_i).$$

This implies

$$\text{BA}(X_1, ..., X_k) - \frac{1}{k} \leq \frac{k-1}{k}\text{BA}(X_1, ..., X_{k-1}) \leq \text{BA}(X_1, ..., X_k).$$

i.e. conditional on $(X_1, ..., X_{k-1})$, BA_k is supported on an interval of size $1/k$. Therefore,

$$\text{Var}[\text{BA}|X_1, ..., X_{k-1}] \leq \frac{1}{4k^2}$$

since $\frac{1}{4c^2}$ is the maximal variance for any r.v. with support of length c. $\square$

2.5.1 Inference of average Bayes accuracy

2.5.2 Classification without model selection

Recall the notation used in section 2.1: the k stimuli exemplars are denoted $\{x^{(1)}, ..., x^{(k)}\}$ and the r responses for the ith class are given by $y^{(i),1}, ..., y^{(i),r}$.

Recall that *data-splitting*, one creates a *training set* consisting of r_1 repeats per class,

$$\{(x^{(1)}, y^{(1),1}), ..., (x^1, y^{(1),r_1}), ..., (x^{(k)}, y^{(k),1}), ..., (x^{(m)}, y^{(m),r_1})\}$$

and a *test set* consisting of the remaining $r_2 = r - r_1$ repeats.

$$\{(x^{(1)}, y^{(1),r_1+1}), ..., (x^{(1)}, y^{(1),r}), ..., (x^{(k)}, y^{(k),r_1+1}), ..., (x^{(k)}, y^{(k),r_1})\}.$$

One inputs the training data into the classifier to obtain the classification rule f,

$$f = \mathcal{F}(\{(x^{(1)}, y^{(1),1}), ..., (x^{(1)}, y^{(1),r_1}), ..., (x^{(k)}, y^{(k),1}, ..., (x^{(k)}, y^{(k),r_1})\}).$$

The test statistic of interest is the test error, defined as

$$\widehat{\text{GA}} = \frac{1}{kr_2} \sum_{i=1}^{k} \sum_{j=r_1+1}^{r} \text{I}(f(y^{(i),j}) \neq i).$$

Since $kr_2\widehat{GA}$ is a sum of independent binary random variables, from Hoeffding's inequality, we have

$$\Pr[\widehat{GA} > GA + \frac{t}{kr_2}] \le 2e^{-2kr_2t^2}.$$

Therefore,

$$\underline{GA}_\alpha = \widehat{GA} - \sqrt{\frac{-\log(\alpha/2)}{2kr_2}}$$

is a $(1-\alpha)$ lower confidence bound for $GA(f)$. But, since

$$GA(f) \le BA(x^{(1)}, \dots, x^{(k)}),$$

it follows that $\underline{GA}_\alpha$ is also a $(1-\alpha)$ lower confidence bound for $BA(x^{(1)}, \dots, x^{(k)})$.

Next, consider the variance bound for BA. From Chebyshev's inequality,

$$\Pr[|BA(X^{(1)}, \dots, X^{(k)}) - ABA_k| > \frac{1}{\sqrt{4\alpha k}}] \le \alpha.$$

Combining these facts, we get the following result.

Theorem 2.5.2 *The following is a $(1-\alpha)$ lower confidence bound for ABA_k:*

$$\underline{ABA}_k = \widehat{GA} - \sqrt{\frac{-\log(\alpha/4)}{2kr_2}} - \frac{1}{\sqrt{2\alpha k}}.$$

That is, for all joint densities $p(x, y)$,

$$\Pr[\underline{ABA}_K > ABA_k] \le \alpha.$$

Proof. Suppose that both $BA(X^{(1)}, \dots, X^{(k)}) \le ABA_k + \frac{1}{\sqrt{2\alpha k}}$ and $\underline{GA}_{\alpha/2} \le GA$. Then it follows that

$$\underline{GA}_{\alpha/2} \le BA(X^{(1)}, \dots, X^{(k)}) \le ABA_k + \frac{1}{\sqrt{2\alpha k}}$$

and hence

$$\underline{ABA}_k = \underline{GA}_{\alpha/2} - \frac{1}{\sqrt{2\alpha k}} \le ABA_k.$$

Therefore, in order for a type I error to occur, either $BA(X^{(1)}, \dots, X^{(k)}) > ABA_k + \frac{1}{\sqrt{2\alpha k}}$ or $\underline{GA}_{\alpha/2} > GA$. But each of these two events has probability of at most $\alpha/2$, hence the union of the probabilities is at most α. $\square$

2.5.3 Classification with model selection

In practice, it is common to evaluate multiple classifiers on the test set, ultimately *selecting* the classifier with the best test performance. Due to selection, the test accuracy $\widehat{GA}$ of the selected classifier becomes biased upwards with respect to the true generalization accuracy. Nevertheless, we can correct for the selection effect using the Bonferroni correction.

Suppose the investigator begins with classifiers $\mathcal{F}_1, \dots, \mathcal{F}_\ell$, and obtains corresponding classification rules $f_1, \dots, f_\ell$ via

$$f_i = \mathcal{F}_i(\{(x^{(1)}, y^{(1),1}), \dots, (x^{(1)}, y^{(1),r_1}), \dots, (x^{(k)}, y^{(k),1}), \dots, (x^{(k)}, y^{(k),r_1})\}).$$

for $i = 1, \ldots, \ell$. Next, they evaluate the test accuracies $\widehat{GA}(f_i)$ according to (**??**). Since $BA(x^{(1)}, \ldots, x^{(k)}) \geq \max_i GA(f_i)$, we have the following lemma.

Lemma 2.5.1 *The following is a $(1 - \alpha)$ lower confidence bound for $BA(x^{(1)}, \ldots, x^{(k)})$:*

$$\underline{BA}_\alpha(x^{(1)}, \ldots, x^{(k)}) = \max_{i=1}^{\ell} \underline{GA}_{\alpha/\ell}(f_i) = \max_{i=1}^{\ell} \widehat{GA}(f_i) - \sqrt{\frac{-\log(\alpha/(2\ell))}{2kr_2}}.$$

Proof. In order for type I error to occur, $\underline{GA}_{\alpha/\ell}(f_i) \geq BA(x^{(1)}, \ldots, x^{(k)}) \geq GA(f_i)$ for some $i = 1, \ldots, \ell$. For each i, the event occurs with probability at most α/ℓ. Therefore, by the union bound, the probability of type I error is at most α. $\square$

It remains to apply the variance bound for Bayes accuracy to obtain a lower confidence bound for ABA_k:

$$\underline{ABA}_k = \underline{BA}_{\alpha/2} - \frac{1}{\sqrt{2\alpha k}}$$

2.6   Identification task

The identification task originated as a method for evaluating the quality of encoding models in neuroscience (Kay 2008).

2.6.1   Experimental design

We consider experiments in which a single subject is presented with a sequence of T stimuli: each stimulus is presented during a 'task window' of a fixed duration. The stimuli are represented by real-valued feature vectors $\vec{X}$; let p be the dimensionality of the feature space. The brain activity of the subject is recorded, yielding a q-dimensional vector $\vec{Y}$: in practice, $\vec{Y}$ could consist of discretized time series data or mean firing rates for spike-sorted neurons, or BOLD response for voxels, depending on the recording modality. Let $\vec{X}^{(t)}$ denote the feature vector of the stimulus, and let $\vec{Y}^{(t)}$ denote the vector of intensities (e.g. BOLD response, mean spike) for the tth task window in the sequence.

2.6.2   Data splitting

The T stimulus-response pairs $(\vec{X}, \vec{Y})$ are randomly partitioned into a *training set* of size N and a *test set* of size $M = T - N$. Form the $N \times p$ data matrix $\boldsymbol{X}^{tr}$ by stacking the features of the N training set stimuli as row vectors, and stack the corresponding responses as row vectors to form the $N \times q$ matrix $\boldsymbol{Y}^{tr}$. Similarly, define $\boldsymbol{X}^{te}$ as the $N \times p$ matrix of test stimuli and $\boldsymbol{Y}^{te}$ as the $N \times q$ matrix of corresponding test responses.

2.6.3   Probabilistic encoding model

The data is used to estimate a stimulus-based encoding model Kay et al. 2008Naselaris et al. 2011Mitchell et al. 2008. The conditional mean response $\mathbf{E}[\boldsymbol{Y}|\boldsymbol{X}]$ is modelled as a linear transformation of the stimulus features,

$$\vec{Y} = \boldsymbol{B}^T \vec{X} + \boldsymbol{\epsilon}$$

where $\boldsymbol{B}$ is a $p \times q$ coefficient matrix and $\boldsymbol{\epsilon}$ is a noise variable with an assumed multivariate normal distribution, $\boldsymbol{\epsilon} \sim N(0, \Sigma)$. Hence, the conditional density of $\vec{Y} | \vec{X}$ is given by the multivariate normal density

$$p(\vec{y}|\vec{x}) = -\frac{1}{(2\pi|\Sigma|)^{-q/2}} \exp\left[-\frac{1}{2}(\vec{y} - \boldsymbol{B}^T \vec{x})^T \Sigma^{-1}(\vec{y} - \boldsymbol{B}^T \vec{x})\right].$$

The coefficient B can be estimated from the training set data $(\boldsymbol{X}^{tr}, \boldsymbol{Y}^{tr})$ using a variety of methods for regularized regression, for instance, the elastic net Zou and Hastie 2005, where each column of $\boldsymbol{B} = (\beta_1, \ldots, \beta_q)$ is estimated via

$$\hat{\beta}_i = \text{argmin}_\beta ||\boldsymbol{Y}_i^{tr} - \boldsymbol{X}^{tr}\beta||^2 + \lambda_1||\beta||_1 + \lambda_2||\beta||_2^2,$$

where λ_1 and λ_2 are regularization parameters which can be chosen via cross-validation Hastie, Tibshirani, and Friedman 2009 separately for each column i.

After forming the estimated coefficient matrix $\hat{\boldsymbol{B}} = (\hat{\beta}_1, \ldots, \hat{\beta}_q)$, we estimate the noise covariance Σ via a shrunken covariance estimateLedoit and Wolf 2004Daniels and Kass 2001 from the residuals,

$$\hat{\Sigma} = \frac{1}{N}((1 - \lambda)S + \lambda\text{Diag}(S))$$

where

$$S = (\boldsymbol{Y}^{tr} - \boldsymbol{X}^{tr}\boldsymbol{B})^T(\boldsymbol{Y}^{tr} - \boldsymbol{X}^{tr}\boldsymbol{B}).$$

2.6.4 Converting the encoding model to a decoding model

Bayes' rule can be used to convert a probabilistic encoding model into a decoding model Naselaris et al. 2011. The Bayesian decoding model gives the posterior probability of the stimulus given the response,

$$p(\vec{x}|\vec{y}) = p(\vec{y}|\vec{x})\frac{p(\vec{x})}{p(\vec{y})}.$$

In an *identification task*Kay et al. 2008, a response $\boldsymbol{y}$ is generated by presenting the subject to a stimulus which is randomly chosen from a subset of k stimuli, $S = (\vec{x}^{(1)}, \ldots, \vec{x}^{(k)})$. The decoder is used to select the stimulus in S which is most likely to have generated the response $\boldsymbol{y}$: the performance of the the decoder is measured by the probability of correct identification. In the identification task, the prior probability $p(\vec{x})$ is uniform over the candidate set S. Therefore, the estimated log posterior probability of each candidate stimulus $\vec{x}^{(i)}$ is given by

$$\log \hat{p}(\vec{x}|\vec{y}) = \log \hat{p}(\vec{y}|\vec{x}) + \text{const.} = -\frac{1}{2}(\vec{y} - \hat{\boldsymbol{B}}^T \vec{x})^T \hat{\Sigma}^{-1}(\vec{y} - \hat{\boldsymbol{B}}^T \vec{x}) + \text{const.}$$

where we have elided the inconsequential constant terms. Therefore, the chosen stimulus $\hat{\vec{x}}$ is the stimulus which minimizes the empirical Mahalanobis distance

$$d_{\hat{\Sigma}}(\vec{y}, \hat{\boldsymbol{B}}^T \vec{x}) = (\vec{y} - \hat{\boldsymbol{B}}^T \vec{x})^T \hat{\Sigma}^{-1}(\vec{y} - \hat{\boldsymbol{B}}^T \vec{x})$$

among the stimuli in S, and supposing that the correcty stimulus has index i, the probability of correct identification is

$$\Pr[\text{correct}] = \Pr[d_{\hat{\Sigma}}(\vec{y}, \hat{\boldsymbol{B}}^T \vec{x}^{(i)}) \leq \min_{j \neq i} d_{\hat{\Sigma}}(\vec{y}, \hat{\boldsymbol{B}}^T \vec{x}^{(j)})].$$

2.6.5   Computation of identification accuracy curve

The probability of correct identification varies depending on the choice of stimulus set S. Therefore, to obtain a well-defined measure of decoder precision, we define the k-class *identification risk* as the expected acccuracy when the set S is constructed by drawing $x^{(1)}, \ldots, x^{(k)}$ independently from the prior distribution $p(\vec{x})$.

An unbiased estimate of the k-class identification risk for any $k \leq M$ can be obtained, where M is the number of test observations. The idea is to evaluate the empirical accuracy (the proportion of correct identifications) over all combinations of $\binom{M}{k}$ stimulus subsets S times all k choices for the correct stimulus within S. Yet, this empirical accuracy can be computed without explicitly looping over all $\binom{kM}{k}$ combinations via a computational trick.

Suppose without loss of generality that the indices of the test observations are $i = 1, \ldots, M$. Define

$$M_{i,j} = \log \hat{p}(\vec{x}^{(j)} | \vec{y}^{(i)})$$

Furthermore, define

$$R_{i,j} = \sum_{\ell \neq j} I\{M_{i,\ell} \geq M_{i,j}\}.$$

The computational trick is to look at each combination of test response $\vec{y}^{(i)}$ and stimulus $\vec{x}^{(\ell)}$, and to count count the number of subsets $N_{i,\ell}$ where (i) both i and ℓ are included in S, and (ii) $\hat{x}^{(i)} = \vec{x}^{(\ell)}$. One can then verify that the empirical accuracy over all subsets is equal to

$$\text{EmpAcc}_k = 1 - \frac{1}{\binom{M}{k}} \frac{1}{k} \sum_{i=1}^{k} \sum_{\ell \neq i} C_{i\ell} N_{i,\ell}. \tag{2.6}$$

Now it is just a matter of simple combinatorics to compute $N_{i,\ell}$. We require both $\vec{x}^{(i)}$ and $\vec{x}^{(\ell)}$ to be included in S. This implies that if $M_{i,i} > M_{i,\ell}$, then $\vec{x}^{(\ell)}$ will never have the highest margin in any of those subsets, so $N_{i,\ell} = 0$.

Otherwise, there are $R_{i,\ell} - 1$ elements with a lower margin than $\vec{x}^{(\ell)}$. Since $i \neq \ell$, then there are $k - 2$ elements in $S \setminus \{i, \ell\}$, so therefore $N_{i,j,\ell} = \binom{R_{i,j,\ell} - 2}{k-2}$. Therefore, we can write

$$N_{i,\ell} = I\{R_{i,\ell} > R_{i,i}\} \binom{R_{i,\ell} - 2}{k - 2} \tag{2.7}$$

The *identification accuracy curve* is defined as the function which maps $k \in 2, 3, \ldots$ to the k-class identification risk. Therefore, an estimate of a portion of the curve can be obtained by estimating the k-class identification risk for $k = 2, \ldots, M$.

Chapter 3

Extrapolating average accuracy

3.1 Motivation

An algorithm that can use sensory information to automatically distinguish between multiple scenarios has increasingly many applications in modern life. Examples include detecting the speaker from his voice patterns, identifying the author from her written text, or labeling the object category from its image. All these examples can be described as multi-class classification problems: the algorithm observes an input x, and uses the classifier function f to guess the label y from a discrete set $\mathcal{Y}$ of possible labels. In all applications described above, the space of potential labels is practically infinite. But in any particular experiment, the number of different labels k used would be finite. A natural question, then, is how changing the number of possible labels affects the classification accuracy.

More technically, we consider a sequence of classification problems on finite label subsets $\mathcal{S}_1 \subset \cdots \subset \mathcal{S}_K \subset \mathcal{Y}$, where in the i-th problem, one constructs the classification rule $f^{(i)} : \mathcal{X} \to \mathcal{S}_i$. Supposing that (X, Y) have a joint distribution, define the misclassification error for the i-th problem as

$$\mathrm{Err}^{(i)} = \Pr[f^{(i)}(X) \neq Y | Y \in \mathcal{S}_i].$$

The problem of *performance extrapolation* is the following: using data from only $\mathcal{S}_k$, can one predict the misclassification error on the larger label set $\mathcal{S}_K$, with $K > k$? Note that unlike other extrapolations from a smaller sample to a larger population, the classification problem becomes harder as the number of distractor classes increases.

Accurate answers to this problem are not only of theoretical interest, but also have practical implications:

- Example 1: A researcher develops a classifier for the purpose of labelling images in 10,000 classes. However, for a pilot study, her resources are sufficient to tag only a smaller subset of these classes, perhaps 100. Can she estimate how well the algorithm work on the full set of classes based on an initial "pilot" subsample of class labels?

- Example 2: A neuroscientist is interested in how well the brain activity in various regions of the brain can discriminate between different classes of stimuli. Kay et al. [1] obtained fMRI brain scans which record how a single subject's visual cortex responds to natural images. They wanted to know how well the brain signals could discriminate between different images. For a set of 1750 photographs, they constructed a classifier which achieved over 0.75 accuracy of classification. Based on exponential extrapolation, they estimate that it would take on the order of $10^{9.5}$ classes before the accuracy of the model

drops below 0.10! A theory of performance extrapolation could be useful for the purpose of making such extrapolations in a more principled way.

- The stories just described can be viewed as a metaphor for typical paradigm of machine learning research, where academic researchers, working under limited resources, develop novel algorithms and apply them to relatively small-scale datasets. Those same algorithms may then be adopted by companies and applied to much larger datasets with many more classes. In this scenario, it would be convenient if one could simply assume that performance on the smaller-scale classification problems was highly representative of performance on larger-scale problems.

Previous works have shown that generalizing from a small set of classes to a larger one is not straightforward. In a paper titled "What does classifying more than 10,000 Image Categories Tell Us," Deng and co-authors compared the performance of four different classifiers on three different scales: a small-scale (1,000-class) problem, medium-scale (7,404-class) problem, and large-scale (10,184-class) problem (all from ImageNet.) They found that while the nearest-neighbor classifier outperformed the support vector machine classifier (SVM) in the small and medium scale, the ranking switched in the large scale, where the SVM classifier outperformed nearest-neighbor. As they write in their conclusion, "we cannot always rely on experiments on small datasets to predict performance at large scale." Theory for performance extrapolation may therefore reveal models with bad scaling properties in the pilot stages of development.

Our primary goal in this paper is to formulate this question, and identify scenarios where answers are possible. The most important condition is that the smaller problem would be representative of the larger one. For simplicity, we assume that in both $\mathcal{S}_K$ and $\mathcal{S}_k$ are iid samples from a population (or distribution) of labels. (Other sampling mechanisms would require some modification). The condition of i.i.d. sampling of labels ensures that the separation of labels in a random set $\mathcal{S}_K$ can be inferred by looking at the empirical separation in $\mathcal{S}_k$, and therefore that some estimate of the achievable accuracy on $\mathcal{S}_K$ can be obtained.

Our analysis considers a restricted set of classifiers, *marginal classifiers*, which train a separate model for each class. This convenient property allows us to characterize the accuracy of the classifier by selectively conditioning on one class at a time. In section **??**, we use this technique to reveal that the expected risk for classifying on the label set $\mathcal{Y}_k$, for all k, is governed by a specific function - the *conditional risk* - that depends on the true distributions and the classifier. As long as one can recover the conditional risk function $\bar{D}(u)$, one can compute the average risk for any number of classes. In section 5, we empirically study the performance curves of classifiers on sequences of classification tasks. Since marginal classifiers only comprise a minority of the classifiers used in practice, we applied our methods to a variety of marginal and non-marginal classifiers in simulations and in one OCR dataset. Our methods have varying success on marginal and non-marginal classifiers, but seem to work badly for neural networks.

Our contribution.

To our knowledge, we are the first to formalize the problem of prediction extrapolation. We develop a general theory for prediction extrapolation under *general class priors* and under bounded cost functions. [[TODO: mention estimation results, theory]]

3.1.1 Facial recognition example

3.2 Assumptions

Implicit in our definition of performance extrapolation is that the new set of k_2 is partially or fully unknown at the time of the extrapolation. Therefore, the extrapolation must account also for the randomness in the choice of labels. We will assume that the labels in the two classification tasks are comparable.

Assumption 1 Let $\mathcal{S}_{k_1}, \mathcal{S}_{k_2}$ be the label sets for the first and second classification tasks. Then $\mathcal{S}_{k_1}, \mathcal{S}_{k_2}$ are i.i.d. samples from an infinite population π.

> **Comments:**
>
> 1. These assumption are most easily satisfied by taking $\mathcal{Y}$ to be a continuous space and letting π be a density over $\mathcal{Y}$. However, a discrete space with a small enough probability for the classes would work well.
>
> 2. Note that here we assumed that the label subsets $\mathcal{S}_{k_1}$ and $\mathcal{S}_{k_2}$ are independent and disjoint. An alternative assumption would be that $\mathcal{S}_{k_1} \subset \mathcal{S}_{k_2}$ with $\mathcal{S}_{k_1}$ being a subsample of $\mathcal{S}_{k_2}$: this assumption can also be addressed, as we will discuss later.
>
> 3. In practice, $\mathcal{S}_{k_1}$ is often a convenience sample meant to be similar to $\mathcal{S}_{k_2}$. The theory will be relevant insofar as the assumptions approximate well the true sampling similarity between the $\mathcal{S}_{k_1}$ and $\mathcal{S}_{k_2}$.
>
> 4. We can imagine other sampling mechanisms designed to make $\mathcal{S}_{k_1}$ a representative sample from the population, e.g. by stratifying. In this paper we do not discuss these more complex sampling schemes.

Our analysis will also rely on a property of the classification model. We do not want the classifier to rely too strongly on complicated interactions between the labels in the set. We therefore propose the following property of marginal separability for classification models:

Definition 3.2.1 *1. The classification rule f is called a* marginal rule *if*

$$f(x) = argmax_{y \in \mathcal{S}} m_y(x),$$

where the function m_y maps $\mathcal{X}$ to $\mathbb{R}$.

2. Define a marginal model $\mathcal{M}$ as a mapping from empirical distributions to margin functions,
$$\mathcal{M}(\hat{F}_y) = m_y(x).$$

3. A classifier that produces marginal classification rules

$$f(x) = argmax_{y \in \mathcal{S}} m_y(x),$$

by use of a marginal model, i.e. such that $m_y = \mathcal{M}(\hat{F}_y)$ for some marginal model $\mathcal{M}$, is called a marginal classifier.

In words, a marginal classification rule produces a *margin*, or score, for each label, and chooses the label with the highest margin. The marginal model converts empirical distributions $\hat{F}_y$ over $\mathcal{X}$ into the margin function m_y. The *marginal* property allows us to prove strong results about the accuracy of the classifier under i.i.d. sampling assumptions.

Comments:

1. The marginal model includes several popular classifiers. A primary example for a marginal model is the estimated Bayes classifier. Let $\hat{f}_y$ be a density estimate obtained from the empirical distribution $\hat{F}_y$. Then, we can use the estimated densities of each class to produce the margin functions:

$$m_y^{EB}(x) = \log(\hat{f}_y(x)).$$

   The resulting empirical approximation for the Bayes classifier (further assuming a uniform prior π) would be

$$f^{EB}(x) = \text{argmax}_{y \in \mathcal{S}}(m_y^{EB}(x)).$$

2. Both the Quadratic Discriminant Analysis and the naive Bayes classifiers can be seen as specific instances of an estimated Bayes classifier [1]. For QDA, the margin function is given by

$$m_y^{QDA}(x) = -(x - \mu(\hat{F}_y))^T \Sigma(\hat{F}_y)^{-1}(x - \mu(\hat{F}_y)) - \log \det(\Sigma(\hat{F}_y)),$$

   where $\mu(F) = \int y \, dF(y)$ and $\Sigma(F) = \int (y - \mu(F))(y - \mu(F))^T dF(y)$. In Naive Bayes, the margin function is

$$m_y^{NB}(x) = \sum_{i=1}^{n} \log \hat{f}_{y,i}(x),$$

   where $\hat{f}_{y,i}$ is a density estimate for the i-th component of $\hat{F}_y$.

3. There are also many classifiers which do not satisfy the marginal property, such as multinomial logistic regression, multilayer neural networks, decision trees, and k-nearest neighbors.

3.3   Analysis of average risk

The result of our analysis is to expose the average risk $\text{AvRisk}_{k,r}$ as the weighted average of a function $\bar{D}(u)$, where $\bar{D}(u)$ is independent of k, and where k only changes the weighting. The result is stated as follows.

Theorem 3.3.1 *Suppose π, $\{F_y\}_{y \in \mathcal{Y}}$ and marginal classifier $\mathcal{F}$ satisfy the tie-breaking condition. Then, under the definitions* (3.2), (3.5), *and* (3.6), *we have*

$$\text{AvRisk}_{k,r} = (k - 1) \int \bar{D}(u) u^{k-2} du. \tag{3.1}$$

---

[1]QDA is the special case of the estimated Bayes classifier when $\hat{f}_y$ is obtained as the multivariate Gaussian density with mean and covariance parameters estimated from the data. Naive Bayes is the estimated Bayes classifier when $\hat{f}_y$ is obtained as the product of estimated componentwise marginal distributions of $p(x_i|y)$

The tie-breaking condition referred in the theorem is defined as follows.

- *Tie-breaking condition*: for all $x \in \mathcal{X}$, $\mathcal{M}(\hat{F}_Y)(x) = \mathcal{M}(\hat{F}_{Y'})(x)$ with zero probability for Y, Y' independently drawn from π.

The tie-breaking condition is a technical assumption which allows us to neglect the specification of a tie-breaking rule in the case that margins are tied. In practice, one can simply break ties randomly, which is mathematically equivalent to adding a small amount of random noise ϵ to the function $\mathcal{M}$.

Our strategy is to analyze the average risk (2.1) by means of *conditioning on* the true label and its training sample, $(y^*, \hat{F}_{y^*})$, and the test feature x^* while *averaging* over all the other random variables. Define the *conditional average risk* $\mathrm{CondRisk}_k((y^*, \hat{F}_{y^*}), x^*)$ as

$$\mathrm{CondRisk}_k((y^*, \hat{F}_{y^*}), x^*) = \mathbf{E}[L | Y^* = y^*, X^* = x^*, \hat{F}_{Y^*} = \hat{F}_{y^*}].$$

Figure 3.1 illustrates the variables which are fixed under conditioning and the variables which are randomized. Compare to figure 2.4.

Without loss of generality, we can write the label subset $\mathcal{S} = \{Y^*, Y^{(1)}, \ldots, Y^{(k-1)}\}$. Note that due to independence, $Y^{(1)}, \ldots, Y^{(k-1)}$ are still i.i.d. from π even conditioning on $Y^* = y^*$. Therefore, the conditional risk can be obtained via the following alternative order of randomizations:

C0. Fix y^*, $\hat{F}_y^*$, and x^*. Note that $M_{y^*}(x^*) = \mathcal{M}(\hat{F}_{y^*})(x^*)$ is also fixed.

C1. Draw the *incorrect labels* $Y^{(1)}, \ldots, Y^{(k)}$ i.i.d. from π. (Note that $Y^{(i)} \neq y^*$ with probability 1 due to the continuity assumptions on $\mathcal{Y}$ and π.)

C2. Draw the training samples for the incorrect labels $\hat{F}_{Y^{(1)}}, \ldots, \hat{F}_{Y^{(k-1)}}$. This determines

$$\hat{Y} = \mathrm{argmax}_{y \in \mathcal{S}} M_y(x^*)$$

and hence

$$L = C(\hat{Y}, y^*).$$

Compared to four randomization steps listed in section **??**, we have essentially conditioned on steps A3 and A4 and randomized over steps A1 and A2.

Now, in order to analyze the k-class behavior of the conditional average risk, we begin by considering the *two-class* situation.

In the two-class situation, we have a true label y^* and one incorrect label, Y. Define the *U-function* $U_{x^*}(y^*, \hat{F}_{y^*})$ as the *probability of correct classification* in the two-class case. The classification is correct if the margin $M_{y^*}(x^*)$ is greater than the margin $M_Y(x^*)$, and incorrect otherwise. Since we are fixing x^* and $(y^*, \hat{F}_{y^*})$, the probability of correct classification is obtained by taking an expectation:

$$U_{x^*}(y^*, \hat{F}_{y^*}) = \Pr[M_{y^*}(x^*) > \mathcal{M}(\hat{F}_Y)(x^*)] \tag{3.2}$$

$$= \int_{\mathcal{Y}} I\{M_{y^*}(x^*) > \mathcal{M}(\hat{F}_y)(x)\} d\Pi_{y,r}(\hat{F}_y) d\pi(y). \tag{3.3}$$

See also figure 3.2 for an graphical illustration of the definition.

An important property of the U-function, and the basis for its name, is that the random variable $U_x(Y, \hat{F}_Y)$ for $Y \sim \pi$ and $\hat{F}_Y \sim \Pi_{Y,r}$ is uniformly distributed for all $x \in \mathcal{X}$. This is proved in Lemma **??** in the appendix.

Now, we will see how the U-function allows us to understand the k-class case. Suppose we have true label y^* and incorrect labels $Y^{(1)}, \ldots, Y^{(k-1)}$. Note that the
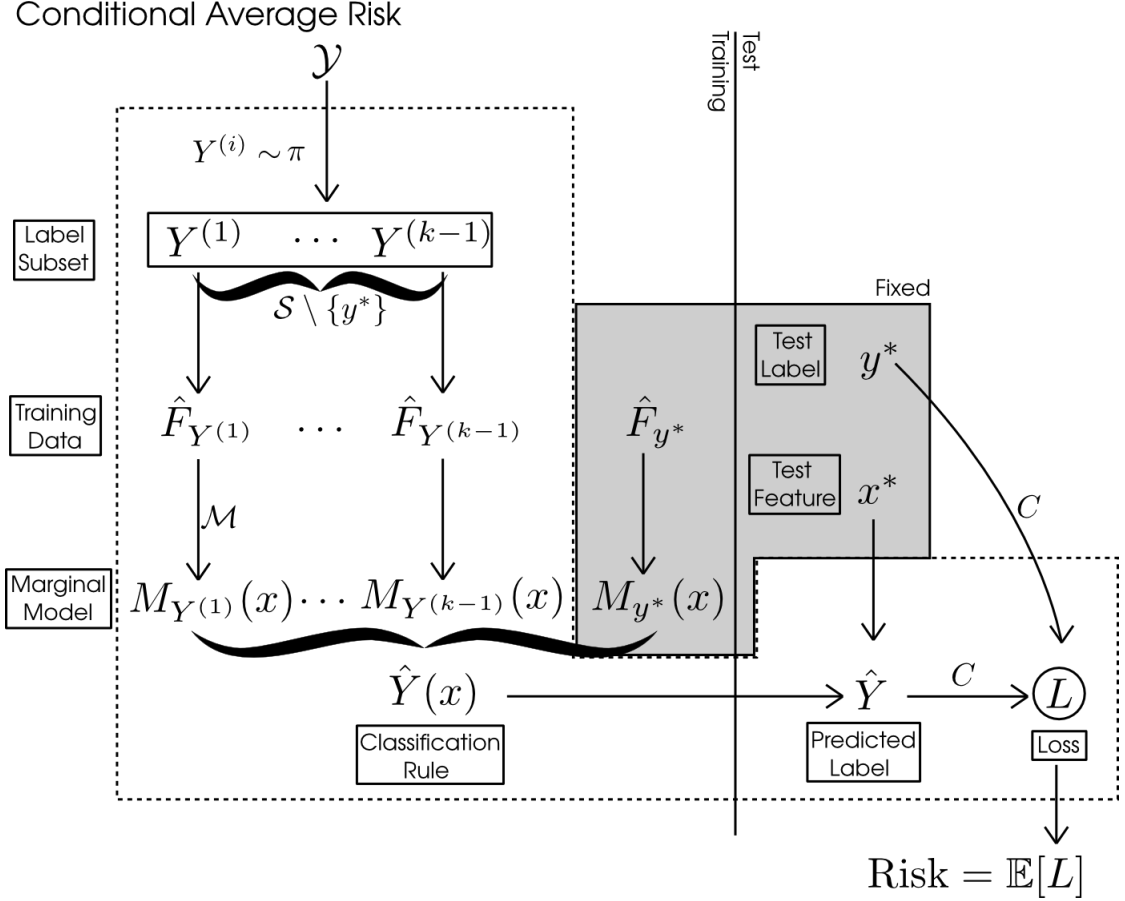
Conditional Average Risk

FIGURE 3.1: Conditional average risk

U-function $U_{x^*}(y, \hat{F}_y)$ is monotonic in $M_y(x^*)$. Therefore,

$$\hat{Y} = \text{argmax}_{y \in \mathcal{S}} M_y(x^*) = \text{argmax}_{y \in \mathcal{S}} U_{x^*}(y, \hat{F}_y).$$

Therefore, we have a correct classification if and only if the U-function value for the correct label is greater than the maximum U-function values for the incorrect labels:

$$\Pr[\hat{Y} = y^*] = \Pr[U_{x^*}(y^*, \hat{F}_{y^*}) > \max_{i=1}^{k-1} U_{x^*}(Y^{(i)}, \hat{F}_{Y^{(i)}})] = \Pr[u^* > U_{max}].$$

where $u^* = U_{x^*}(y^*, \hat{F}_{y^*})$ and $U_{max,k-1} = \max_{i=1}^{k-1} U_{x^*}(Y^{(i)}, \hat{F}_{Y^{(i)}})$. But now, observe that we know the distribution of $U_{max,k-1}$! Since $U_{x^*}(Y^{(i)}, \hat{F}_{Y^{(i)}})$ are i.i.d. uniform, we know that

$$U_{max,k-1} \sim \text{Beta}(k - 1, 1). \tag{3.4}$$

We now have the insights needed to analyze the simplest special case: zero-one loss.

Special case: 0-1 loss. For zero-one loss, which is $C(y, y') = I\{y = y'\}$, we have $L = 1$ if and only if $U_{max} > u^*$ and $L = 0$ otherwise. Therefore, the conditional average risk is

$$\text{CondRisk}_k((y^*, \hat{F}_{y^*}), x^*) = \Pr[U_{max} > u^*] = \int_{u^*}^1 (k - 1)u^{k-2} du.$$

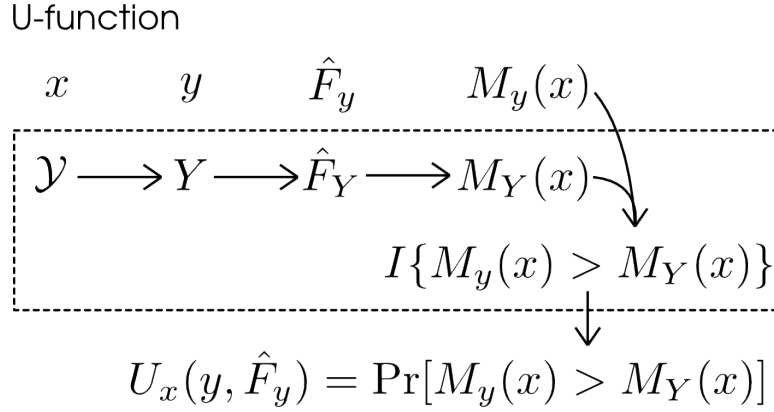U-function

$$U_x(y, \hat{F}_y) = \Pr[M_y(x) > M_Y(x)]$$

FIGURE 3.2: U-functions

Now the average risk can be obtained by integrating over the distribution of $U^* = U_{x^*}(y^*, \hat{F}_{y^*})$. We have

$$\text{AvRisk}_k = \mathbf{E}[\int_{U^*}^1 (k-1)u^{k-2}du]$$

$$= \mathbf{E}[\int_0^1 I\{u \geq U^*\}(k-1)u^{k-2}du]$$

$$= (k-1)\int_0^1 \Pr[U^* \leq u]u^{k-2}du.$$

Or equivalently,

$$\text{AvRisk}_{k,r,\nu}((y^*, \hat{F}_{y^*}), x^*) = (k-1)\int \bar{D}(u)u^{k-2}du.$$

where $\bar{D}(u)$ denote the cumulative distribution function of U^* on $[0, 1]$:

$$\bar{D}(u) = \Pr[U_{x^*}(y^*, \hat{F}_{y^*}) \leq u].$$

We have expressed the average risk expressed as a weighted integral of a certain function $\bar{D}(u)$ defined on $u \in [0, 1]$. We have clearly isolated the part of the average risk which is independent of k–the univariate function $\bar{D}(u)$, and the part which is dependent on k–which is the density of U_{max}.

In section **??**, we will develop estimators of $\bar{D}(u)$ in order to estimate the k-class average risk. But now let us return to the general case.

General loss functions. The case for general cost functions is somewhat more complicated, since knowledge of U_{max} is not sufficient to determine L. In short, this is because U_{max} by itself is insufficient to determine $\hat{Y}$, and therefore $L = C(\hat{Y}, y^*)$. However, we can resolve this issue by noting that for the purposes of computing the expected loss, it suffices to have the *conditional distribution* of $\hat{Y}$ given U_{max}. Even though U_{max} does not deterministically map onto a unique $\hat{Y}$, it determines a conditional distribution of $\hat{Y}$ which allows us to compute $\mathbf{E}[L|U_{max}, x^*, y^*, \hat{F}_{y^*}]$.

Now, a key fact is that the conditional distribution of $\hat{Y}$ given U_{max} *does not depend* on k. To see this fact, suppose without loss of generality that $\hat{Y} = Y^{(k-1)}$. Then the

joint density of $Y^{(1)}, \ldots, Y^{(k-1)}$ given $U_{max} = u$ can be written

$$p(y^{(1)}, \ldots, y^{(k-1)}) \propto \pi(y^{(k-1)}) \frac{d}{dt} \Pr[U_{x^*}(y^{(k-1)}, \hat{F}_{y^{(k-1)}}) \leq t]|_{t=u} \prod_{i=1}^{k-2} \pi(y^{(i)}) \Pr[U_{x^*}(y^{(k-1)}, \hat{F}_{y^{(k-1)}}) < u].\}$$

up to a normalizing constant. Note that the term $\frac{d}{dt} \Pr[U_{x^*}(y^{(k-1)}, \hat{F}_{y^{(k-1)}}) \leq t]$ is the density of the random variable $U_{x^*}(Y^{(k-1)}, \hat{F}_{Y^{(k-1)}})$. From the density, we can see that $Y^{(1)}, \ldots, Y^{(k-1)}$ are conditionally independent given $U_{max} = u$, hence the marginal density of $\hat{Y} = Y^{(k-1)}$ can be written

$$p(\hat{y}) \propto \pi(\hat{y}) \frac{d}{dt} \Pr[U_{x^*}(y^{(k-1)}, \hat{F}_{y^{(k-1)}}) \leq t]|_{t=u}.$$

The only property of the conditional distribution of $\hat{Y}|U_{max} = u$ that is needed is the expectation of $L = C(\hat{Y}, y^*)$. Therefore, define the *conditional expected loss* $D((y^*, \hat{F}_{y^*}), x^*, u)$ by

$$D((y^*, \hat{F}_{y^*}), x^*, u) = \begin{cases} 0 \text{ if } u < u^* \\ \mathbf{E}[C(\hat{Y}, y^*)|U_{max} = u, x^*, y^*, \hat{F}_{y^*}] \text{ otherwise.} \end{cases} \tag{3.5}$$

We have the two cases $u < u^*$ and $u > u^*$ since when $U_{max} < u^*$, the correct label is chosen and the loss is zero. Otherwise, an incorrect label is chosen, and the expected loss must be calculated using the conditional distribution of $\hat{Y}$.

Again, since the conditional distribution of $\hat{Y}|U_{max}, x^*, (y^*, \hat{F}_{y^*})$ is independent of k, the conditional cost function is also independent of k.

With the conditional cost function and the distribution of U_{max} both in hand, we can compute the average conditional risk

$$\text{CondRisk}_k((y^*, \hat{F}_{y^*}), x^*) = (k - 1) \int D((y^*, \hat{F}_{y^*}), x^*, u) u^{k-2} du.$$

Now the average risk can be obtained by integrating over $(Y^*, \hat{F}_{Y^*})$, and X^*.

$$\text{AvRisk}_{k,r} = (k - 1) \int \bar{D}(u) u^{k-2} du.$$

where

$$\bar{D}(u) = \int D((y^*, \hat{F}_{y^*}), x^*, u) \pi(y^*) dy dF_{y^*}(x^*) d\Pi_{y^*,r}(\hat{F}_{y^*}). \tag{3.6}$$

This is the key result behind our estimation method, which was stated in theorem 3.3.1. The proof is given in the appendix.

Having this theoretical result allows us to understand how the expected k-class risk scales with k in problems where all the relevant densities are known. However, applying this result in practice to estimate Average Risk$_k$ requires some means of estimating the unknown function $\bar{D}$–which we discuss in the following.

3.4   Estimation

Now we address the problem of estimating $\text{AvRisk}_{k_2, r_{train}}$ from data. As we have seen from Theorem 3.3.1, the k-class average risk of a marginal classifier $\mathcal{M}$ is a functional of a object called $\bar{D}(u)$, which depends marginal model $\mathcal{M}$ of the classifier,

the joint distribution of labels Y and features X when Y is drawn from the sampling density ν.

Therefore, the strategy we take is to attempt to estimate $\bar{D}$ for then given classification model, and then plug in our estimate of $\bar{D}$ into the integral (3.1) to obtain an estimate of $\text{AvRisk}_{k_2, r_{train}}$.

Having decided to estimate $\bar{D}$, there is then the question of what kind of model we should assume for $\bar{D}$. While a nonparametric approach may be ideal, for the case of general loss functions we will adopt a parametric model: that is the subject of this section.

Let us assume the linear model

$$\bar{D}(u) = \sum_{\ell=1}^{m} \beta_\ell h_\ell(u), \tag{3.7}$$

where $h_\ell(u)$ are known basis functions, and β are the model parameters to be estimated. We can obtain *unbiased* estimation of $\text{AvRisk}_{k_2, r_{train}}$ via the unbiased estimates of k-class average risk obtained from (2.6).

If we plug in the assumed linear model (3.7) into the identity (3.1), then we get

$$\text{AvRisk}_{k, r_{train}} = (k-2) \int \bar{D}(u) u^{k-2} du \tag{3.8}$$

$$= (k-2) \int_0^1 \sum_{\ell=1}^{m} \beta_\ell h_\ell(u) u^{k-2} du \tag{3.9}$$

$$= \sum_{\ell=1}^{m} \beta_\ell H_{\ell, k} \tag{3.10}$$

where

$$H_{\ell, k} = (k-2) \int_0^1 h_\ell(u) u^{k-2} du. \tag{3.11}$$

The constants $H_{\ell, k}$ are moments of the basis function h_ℓ: hence we call this method the *moment method.* Note that $H_{\ell, k}$ can be precomputed numerically for any $k \geq 2$.

Now, since the AvTestRisk_k are unbiased estimates of $\text{AvRisk}_{k, r_{train}}$, this implies that the regression estimate

$$\hat{\beta} = \text{argmin}_\beta \sum_{k=2}^{k_1} w_k \left(\text{AvTestRisk}_k - \sum_{\ell=1}^{m} \beta_\ell H_{\ell, k} \right)^2$$

is unbiased for β, under any choice of positive weights w_k. The estimate of $\text{AvRisk}_{k_2, r_{train}}$ is similarly obtained from (3.10), via

$$\widehat{\text{AvRisk}_{k_2, r_{train}}} = \sum_{\ell=1}^{m} \hat{\beta}_\ell H_{\ell, k_2}. \tag{3.12}$$

3.4.1 Large-Sample Theory

How good are the estimated average risks (3.12)? Let us investigate the accuracy of the estimates in the limit where $k_1 \to \infty$, first in the case where the model (3.7) is correctly specified, and then considering possible model misspecification.

If we fix the number of classes k_2 which defines the estimation target, then we need not use the estimator (3.12), since once $k_1 > k_2$, we can use the AvTestRisk_{k_2}

as an estimator instead, which can easily be shown to a have a convergence rate of $O(1/\sqrt{k_1})$ to the true average risk. Therefore, if we want to quantify the performance of the regression-based estimator (3.12), it does not make sense to look at asymptotic settings where k_2 is fixed. One approach is to specify a setting where k_2 changes as a function of k_1. However, the approach we will take is to look at the minimax error: that is, to look at the maximum discrepancy between the estimate and the true average risk over all k_2 simultaneously. The performance criterion is the minimax error, defined

$$\text{MinimaxError} = \sup_{k_2 > 2} |\widehat{\text{AvRisk}_{k_2, r_{train}}} - \text{AvRisk}_{k_2, r_{train}}|. \tag{3.13}$$

Well-specified case.

Let us first assume that the parametric model (3.7) is correct. Then

$$\text{AvRisk}_{k_2, r_{train}} = \sum_{\ell=1}^{m} \beta_\ell H_{\ell, k_2} = \langle \vec{H}_{k_2}, \beta \rangle$$

where $\vec{H}_{k_2} = (H_{\ell, k_2})_{\ell=1}^{m}$. Then, we get

$$\text{MinimaxError} = \sup_{k_2 > 2} |\langle \vec{H}_{k_2}, \beta - \hat{\beta} \rangle|.$$

If we assume that all the basis functions $h_\ell(u)$ are bounded by a common constant M, then it follows that H_ℓ, k are also bounded by the same constant M, and we have

$$\text{MinimaxError} \leq M ||\beta - \hat{\beta}||_1 \leq M \sqrt{m} ||\beta - \hat{\beta}||_2$$

Therefore, any convergence rate we can establish for $\hat{\beta}$ is inherited by the minimax error. Meanwhile, we can show that choosing k_0 sufficiently large that $(\vec{H}_2, \ldots, \vec{H}_{k_0})$ is full-rank, and setting weights $w_k = I\{k \leq k_0\}$, then the resulting $\hat{\beta}$ converges to the true β at the usual $O(1/\sqrt{n})$ rate. We state the result in the following theorem.

Theorem 3.4.1 *Consider a sequence of problems where the model $\mathcal{M}$, r_{train}, r_{test}, joint distribution $\{F_y\}_{y \in \mathcal{Y}}$, and class sampling distribution η are fixed as $k_1 \to \infty$. Further assume that the function $\bar{D}(u)$ defined by $\{F_y\}_{y \in \mathcal{Y}}$, η, and $\mathcal{M}$ satisfies*

$$\bar{D}(u) = \sum_{\ell=1}^{m} \beta_\ell h_\ell(u)$$

for some basis functions $h_\ell(u)$. Let k_0 be an integer sufficiently large so that

$$Rank(\vec{H}_2, \ldots, \vec{H}_{k_0}) = m.$$

Then, defining

$$\hat{\beta} = argmin_\beta \sum_{k=2}^{k_0} \left(AvTestRisk_k - \sum_{\ell=1}^{m} \beta_\ell H_{\ell, k} \right)^2$$

there exists some constant $C < \infty$ such that

$$\lim_{k_1 \to \infty} \sqrt{k_1} ||\hat{\beta} - \beta||_2 = C.$$

Proof. Note that the statistics $AvTestRisk_k$ are U-statistics of the k_1 pairs of test and training samples. Therefore, by Hoeffding 1948, it follows that $(AvTestRisk_2, \ldots, AvTestRisk_{k_0})$

is asymptotically normal with covariance satisfying

$$\lim_{k_1\to\infty} k_1 \text{Cov}(\text{AvTestRisk}_2, \ldots, \text{AvTestRisk}_{k_0}) = \Sigma,$$

for some positive semidefinite matrix Σ. Defining $\boldsymbol{H}$ to be the matrix with rows $\vec{H}_2, \ldots, \vec{H}_{k_0}$, this then implies that

$$\lim_{k_1\to\infty} k_1 \text{Cov}(\hat{\beta}) = (\boldsymbol{H}^T\boldsymbol{H})^{-1}\boldsymbol{H}^T\Sigma\boldsymbol{H}(\boldsymbol{H}^T\boldsymbol{H})^{-1}.$$

It follows that defining

$$C = \sqrt{\text{tr}(\boldsymbol{H}^T\boldsymbol{H})^{-1}\boldsymbol{H}^T\Sigma\boldsymbol{H}(\boldsymbol{H}^T\boldsymbol{H})^{-1}}$$

we have

$$\lim_{k_1\to\infty} \sqrt{k_1}||\hat{\beta} - \beta||_2 = C.$$

$\square$.

Misspecified case.

Now consider the more realistic setting where the model (3.7) is misspecified. We quantify the degree of misspecification by the ℓ_∞ error on [0,1]. Define

$$\delta = \inf_\beta \left\| \bar{D}(u) - \sum_{\ell=1}^m \beta_\ell h_\ell(u) \right\|_\infty,$$

and let $\tilde{\beta}$ be the coefficients β which attain the infimum, with $\tilde{D}(u) = \sum_{\ell=1}^m \tilde{\beta}_\ell h_\ell(u)$. To deal with this case, refer to the theory in section **??**. For each $u = [0,1]$, find a matrix $A(u)$ such that (i) the first column equals

$$A_1(u) = (h_1(u), \ldots, h_m(u))$$

and that (ii) the rest of the columns are orthogonal to the first, and (iii) $A(u)$ is full-rank. Then define $Z(u) = XA(u)$, and consider the column vector

$$Z_{1|-1}(u) = (I - P_{Z_{-1}})Z_1(u).$$

It can be shown that $Z_{1|-1}(u)$ is well-defined, regardless of how $A(u)$ is chosen. Then, by the theory in section **??**, the extra bias due to approximation error for predicting $\hat{D}(u)$ is given by

$$\text{Bias}^2(u) = \frac{||Z_{1|-1}(u)||_1^2}{||Z_{1|-1}(u)||_2^4}.$$

Define the maximum bias as

$$\text{Bias}^2_{max} = \sup_{u\in[0,1]} \text{Bias}^2(u).$$

From the analysis of the well-specified case, we know that the variance component of the prediction risk decreases at order $O(1/k)$. Therefore, the misspecified minimax error is of order

$$\text{MinimaxError} = O(1/\sqrt{k}) + \text{Bias}^2_{max}.$$

3.5 Examples

Chapter 4

Inference of mutual information

4.1 Motivation

4.1.1 Gene expression dataset example

4.2 Identification loss

4.3 Average Bayes accuracy and Mutual information

4.3.1 Problem formulation and result

Let $\mathcal{P}$ denote the collection of all joint densities $p(x, y)$ on finite-dimensional Euclidean space. For $\iota \in [0, \infty)$ define $C_k(\iota)$ to be the largest k-class average Bayes error attained by any distribution $p(x, y)$ with mutual information not exceeding ι:

$$C_k(\iota) = \sup_{p \in \mathcal{P}: \mathrm{I}[p(x,y)] \leq \iota} \mathrm{ABA}_k[p(x, y)].$$

A priori, $C_k(\iota)$ exists since ABA_k is bounded between 0 and 1. Furthermore, C_k is nondecreasing since the domain of the supremum is monotonically increasing with ι.

It follows that for any density $p(x, y)$, we have

$$\mathrm{ABA}_k[p(x, y)] \leq C_k(\mathrm{I}[p(x, y)]).$$

Hence C_k provides an upper bound for average Bayes error in terms of mutual information.

Conversely we have

$$\mathrm{I}[p(x, y)] \geq C_k^{-1}(\mathrm{ABA}_k[p(x, y)])$$

so that C_k^{-1} provides a lower bound for mutual information in terms of average Bayes error.

On the other hand, there is no nontrivial *lower* bound for average Bayes error in terms of mutual information, nor upper bound for mutual information in terms of average Bayes error, since

$$\inf_{p \in \mathcal{P}: \mathrm{I}[p(x,y)] \leq \iota} \mathrm{ABA}_k[p(x, y)] = \frac{1}{k}.$$

regardless of ι.

The goal of this work is to attempt to compute or approximate the functions C_k and C_k^{-1}.

In the following sections we determine the value of $C_k(\iota)$, leading to the following result.

Theorem 4.3.1 *For any $\iota > 0$, there exists $c_\iota \geq 0$ such that defining*

$$Q_c(t) = \frac{\exp[ct^{k-1}]}{\int_0^1 \exp[ct^{k-1}]},$$

we have

$$\int_0^1 Q_{c_\iota}(t) \log Q_{c_\iota}(t) dt = \iota.$$

Then,

$$C_k(\iota) = \int_0^1 Q_{c_\iota}(t) t^{k-1} dt.$$

We obtain this result by first reducing the problem to the case of densities with uniform marginals, then doing the optimization over the reduced space.

4.3.2   Reduction

Let $p(x, y)$ be a density supported on $\mathcal{X} \times \mathcal{Y}$, where $\mathcal{X}$ is a subset of $\mathbb{R}^{d_1}$ and $\mathcal{Y}$ is a subset of $\mathbb{R}^{d_2}$, and such that $p(x)$ is uniform on $\mathcal{X}$ and $p(y)$ is uniform on $\mathcal{Y}$.

Now let $\mathcal{P}^{unif}$ denote the set of such distributions: in other words, $\mathcal{P}^{unif}$ is the space of joint densities in Euclidean space with uniform marginals over the marginal supports. In this section, we prove that

$$C_k(\iota) = \inf_{p \in \mathcal{P}: \mathrm{I}[p(x,y)] \leq \iota} \mathrm{ABA}_k[p(x, y)] = \inf_{p \in \mathcal{P}^{unif}: \mathrm{I}[p(x,y)] \leq \iota} \mathrm{ABA}_k[p(x, y)],$$

thus reducing the problem of optimizing over the space of all densities to the problem of optimizing over densities with uniform marginals.

Also define $\mathcal{P}^{bounded}$ to be the space of all densities $p(x, y)$ with finite-volume support. Since uniform distributions can only be defined over sets of finite volume, we have

$$\mathcal{P}^{unif} \subset \mathcal{P}^{bounded} \subset \mathcal{P}.$$

Therefore, it is necessary to first show that

$$\inf_{p \in \mathcal{P}: \mathrm{I}[p(x,y)] \leq \iota} \mathrm{ABA}_k[p(x, y)] = \inf_{p \in \mathcal{P}^{bounded}: \mathrm{I}[p(x,y)] \leq \iota} \mathrm{ABA}_k[p(x, y)].$$

This is accomplished via the following lemma.

Lemma 4.3.1 *(Truncation). Let $p(x, y)$ be a density on $\mathbb{R}^{d_x} \times \mathbb{R}^{d_y}$. For all $\epsilon > 0$, there exists a subset $\mathcal{X} \subset \mathbb{R}^{d_x}$ with finite volume with respect to d_x-dimensional Lesbegue measure, and a subset $\mathcal{Y} \subset \mathbb{R}^{d_y}$ with finite volume with respect to d_y-dimensional Lesbegue measure, such that defining*

$$\tilde{p}(x, y) = \frac{I\{(x, y) \in \mathcal{X} \times \mathcal{Y}\}}{\int_{\mathcal{X} \times \mathcal{Y}} p(x, y) dx dy} p(x, y),$$

we have

$$|I[p] - I[\tilde{p}]| < \epsilon$$

and

$$|ABA_k[p] - ABA_k[\tilde{p}]| < \epsilon.$$

Proof. Recall the definition of the Shannon entropy H:

$$H[p(x)] = - \int p(x) \log p(x) dx.$$

It is a well-known in information theory that

$$I[p(x, y)] = H[p(x)] + H[p(y)] - H[p(x, y)].$$

There exists a sequence $(\mathcal{X}_i, \mathcal{Y}_i)_{i=1}^{\infty}$ where $(\mathcal{X}_i)_{i=1}^{\infty}$ is an increasing sequence of finite-volume subsets of $\mathbb{R}^{d_x}$ and $(\mathcal{Y}_i)_{i=1}^{\infty}$ is an increasing sequence of finite-volume subsets of $\mathbb{R}^{d_y}$, and $\lim_{i \to \infty} \mathcal{X}_i = \mathbb{R}^{d_x}$, $\lim_{i \to \infty} \mathcal{Y}_j$. Define

$$\tilde{p}_i(x, y) = \frac{I\{(x, y) \in \mathcal{X}_i \times \mathcal{Y}_i\}}{\int_{\mathcal{X}_i \times \mathcal{Y}_i} p(x, y) dx dy} p(x, y)$$

Note that $\tilde{p}_i$ gives the conditional distribution of (X, Y) conditional on $(X, Y) \in \mathcal{X}_i \times \mathcal{Y}_i$. Furthermore, it is convenient to define $\tilde{p}_{\infty} = p$. We can find some i_1, such that for all $i \geq i_1$, we have

$$\left| \int_{x \notin \mathcal{X}_i} p(x) \log p(x) dx \right| < \frac{\epsilon}{6}$$

$$\left| \int_{y \notin \mathcal{Y}_i} p(y) \log p(y) dy \right| < \frac{\epsilon}{6}$$

$$\left| \int_{(x,y) \notin \mathcal{X}_i \times \mathcal{Y}_i} p(x, y) \log p(x, y) dx dy \right| < \frac{\epsilon}{6}$$

and also such that

$$- \log \left[\int_{x,y \in \mathcal{X}_i \times \mathcal{Y}_i} p(x, y) dx dy \right] < \frac{\epsilon}{2}$$

Then, it follows that

$$|I[p] - I[\tilde{p}_i]| < \epsilon$$

for all $i \geq i_1$.

Now we turn to the analysis of average Bayes error. Let f_i denote the Bayes k-class classifier for $\tilde{p}_i(x, y)$ and f_{∞} the Bayes k-class classifier for $p(x, y)$: recall that by definition,

$$\text{ABA}_k[\tilde{p}_i] = \Pr_{\tilde{p}_i}[f_i(X^{(1)}, ..., X^{(k)}, Y) = Z]$$

Define

$$\epsilon_i = \Pr_p[(X^{(1)}, ..., X^{(k)}, Y) \notin \mathcal{X}_i^k \times \mathcal{Y}_i];$$

by continuity of probability we have $\lim_i \epsilon_i \to 0$. We claim that

$$|\text{ABA}_k[\tilde{p}_i] - \text{ABA}_k[p]| \leq \epsilon_i.$$

Given the claim, the proof is completed by finding $i > i_1$ such that $\epsilon_i < \epsilon$, and defining $\mathcal{X} = \mathcal{X}_i$, $\mathcal{Y} = \mathcal{Y}_i$.

Consider using f_i to obtain a classification rule for $p(x, y)$: define

$$\tilde{f}_i = \begin{cases} f_i(x^{(1)}, ..., x^{(k)}, y) & \text{when } (x^{(1)}, ..., x^{(k)}, y) \in \mathcal{X}_i^k \times \mathcal{Y} \\ 0 & \text{otherwise.} \end{cases}$$

We have

$$
\begin{aligned}
\mathrm{ABA}_k[p] =& \sup_f \Pr_p[f(X^{(1)}, ..., X^{(k)}, Y) = Z] \\
\geq& \\
=& (1 - \epsilon_i) \Pr_p[f_i(X^{(1)}, ..., X^{(k)}, Y) = Z | (X^{(1)}, ..., X^{(k)}, Y) \in \mathcal{X}_i^k \times \mathcal{Y}_i] \\
& + \epsilon_i \Pr_p[f_i(X^{(1)}, ..., X^{(k)}, Y) = Z | (X^{(1)}, ..., X^{(k)}, Y) \notin \mathcal{X}_i^k \times \mathcal{Y}_i] \\
=& (1 - \epsilon_i) \Pr_{\tilde{p}}[f_i(X^{(1)}, ..., X^{(k)}, Y) = Z] + \epsilon_i 0 \\
=& (1 - \epsilon_i) \mathrm{ABA}_k[\tilde{p}_i] \geq \mathrm{ABA}_k[\tilde{p}_i] - \epsilon_i.
\end{aligned}
$$

In other words, when $\tilde{p}_i$ is close to p, the Bayes classification rule for $\tilde{p}_i$ obtains close to the Bayes rate when the data is generated under p.

Now consider the reverse scenario of using f_p to perform classification under $\tilde{p}_i$. This is equivalent to generating data under $p(x, y)$, performing classification using f, then only evaluating classification accuracy conditional on $(X^{(1)}, ..., X^{(k)}, Y) \in \mathcal{X}_i^k \times \mathcal{Y}_i$. Therefore,

$$
\begin{aligned}
\mathrm{ABA}_k[\tilde{p}_i] =& \sup_f \Pr_{\tilde{p}_i}[f(X^{(1)}, ..., X^{(k)}, Y) = Z] \\
\geq& \Pr_{\tilde{p}_i}[f_p(X^{(1)}, ..., X^{(k)}, Y) = Z] \\
=& \Pr_p[f_p(X^{(1)}, ..., X^{(k)}, Y) = Z | (X^{(1)}, ..., X^{(k)}, Y) \in \mathcal{X}_i^k \times \mathcal{Y}_i] \\
=& \frac{1}{1 - \epsilon_i} \Pr_p[I\{(X^{(1)}, ..., X^{(k)}, Y) \in \mathcal{X}_i^k \times \mathcal{Y}_i\} \text{ and } f_p(X^{(1)}, ..., X^{(k)}, Y) = Z] \\
\geq& \frac{1}{1 - \epsilon_i} \left(1 - \Pr_p[I\{(X^{(1)}, ..., X^{(k)}, Y) \notin \mathcal{X}_i^k \times \mathcal{Y}_i\}] - \Pr_p[f_p(X^{(1)}, ..., X^{(k)}, Y) \neq Z]] \right) \\
=& \frac{\mathrm{ABA}_k[p] - \epsilon_i}{1 - \epsilon_i} \geq \mathrm{ABA}_k[p] - \epsilon_i.
\end{aligned}
$$

In other words, when $\tilde{p}_i$ is close to p, the Bayes classification rule for p obtains close to the Bayes rate when the data is generated under $\tilde{p}_i$.

Combining the two directions gives $|\mathrm{ABA}_k[\tilde{p}_i] - \mathrm{ABA}_k[p]| \leq \epsilon_i$, as claimed. $\square$

One can go from bounded-volume sets to uniform distributions by adding auxillary variables. To illustrate the intution, consider a density $p(x)$ on a set of bounded volume, $\mathcal{X}$. Introduce a variable W such that conditional on $X = x$, we have w uniform on $[0, p(x)]$. It follows that the joint density $p(x, w) = 1$ and is supported on a set $\mathcal{X}' = \mathcal{X} \times [0, \infty]$. Furthermore, $\mathcal{X}'$ is of bounded volume (in fact, of volume 1) since

$$
\int_{\mathcal{X}'} dx = \int_{\mathcal{X}'} p(x, w) dx = 1.
$$

Therefore, to accomplish the reduction from $\mathcal{P}$ to $\mathcal{P}^{unif}$, we start with a density $p(x, y) \in \mathcal{P}$, and using Lemma 4.3.1, find a suitable finite-volume truncation $\tilde{p}(x, y)$. Finally, we introduce auxillary variables w and z so that the expanded joint distribution $p(x, w, y, z)$ has uniform marginals $p(x, w)$ and $p(y, z)$. However, we still need to check that the introduction of auxillary variables preserves the mutual information and average Bayes error; this is the content of the next lemma.

Lemma 4.3.2 *Suppose X, Y, W, Z are continuous random variables, and that $W \perp Y|Z$, $Z \perp X|Y$, and $W \perp Z|(X, Y)$. Then,*

$$I[p(x, y)] = I[p((x, w), (y, z))]$$

Proof. Due to conditional independence relationships, we have

$$p((x, w), (y, z)) = p(x, y)p(w|x)p(z|y).$$

It follows that

$$
\begin{aligned}
\mathrm{I}[p((x, w), (y, z))] &= \int dxdwdydz\ p(x, y)p(w|x)p(z|w) \log \frac{p((x, w), (y, z))}{p(x, w)p(y, z)} \\
&= \int dxdwdydz\ p(x, y)p(w|x)p(z|w) \log \frac{p(x, y)p(w|x)p(z|y)}{p(x)p(y)p(w|x)p(z|y)} \\
&= \int dxdwdydz\ p(x, y)p(w|x)p(z|w) \log \frac{p(x, y)}{p(x)p(y)} \\
&= \int dxdy\ p(x, y) \log \frac{p(x, y)}{p(x)p(y)} = \mathrm{I}[p(x, y)].
\end{aligned}
$$

Also,

$$
\begin{aligned}
\mathrm{ABA}_k[p((x, w), (y, z))] &= \int \left[\prod_{i=1}^{k} p(x_i, w_i)dx_idw_i \right] \int dydz\ \max_i p(y, z|x_i, w_i). \\
&= \int \left[\prod_{i=1}^{k} p(x_i, w_i)dx_idw_i \right] \int dy\ \max_i p(y|x_i) \int dz\ p(z|y). \\
&= \int \left[\prod_{i=1}^{k} p(x_i)dx_i \right] \left[\prod_{i=1}^{k} \int dw_i p(w_i|x_i) \right] \int dy\ \max_i p(y|x_i) \\
&= \mathrm{ABA}_k[p(x, y)].
\end{aligned}
$$

□

Combining these lemmas gives the needed reduction, given by the following theorem.

Theorem 4.3.2 *(Reduction.)*

$$\inf_{p\in\mathcal{P}:\mathrm{I}[p(x,y)]\leq\iota} ABA_k[p(x, y)] = \inf_{p\in\mathcal{P}^{unif}:\mathrm{I}[p(x,y)]\leq\iota} ABA_k[p(x, y)].$$

The proof is trivial given the previous two lemmas.

4.3.3 Proof of theorem

Proof of theorem 4.3.1

Using Theorem 4.3.2, we have

$$C_k(\iota) = \inf_{p\in\mathcal{P}^{unif}:\mathrm{I}[p(x,y)]\leq\iota} ABA_k[p(x, y)].$$

Define $f(\iota) = \int_0^1 Q_{c_\iota}(t)t^{k-1}dt$: our goal is to establish that $C_k(\iota) = f(\iota)$. Note that $f(\iota)$ is the same function which appears in Lemma **??** and the same bound as established in Lemma **??**.

Define the density $p_\iota(x, y)$ where

$$p_\iota(x, y) = \begin{cases} g_\iota(y - x) & \text{for } x \geq y \\ g_\iota(1 + y - x) & \text{for } x < y \end{cases}$$

where

$$g_\iota(x) = \frac{d}{dx} G_\iota(x)$$

and G_ι is the inverse of Q_c.

One can verify that $I[p_\iota] = \iota$, and

$$\text{ABA}_k[p] = \int_0^1 Q_{c_\iota}(t) t^{k-1} dt.$$

This establishes that

$$C_k(\iota) \geq \int_0^1 Q_{c_\iota}(t) t^{k-1} dt.$$

It remains to show that for all $p \in \mathcal{P}^{unif}$ with $I[p] \leq \iota$, that $\text{ABA}_k[p] \leq \text{ABA}_k[p_\iota]$.

Take $p \in \mathcal{P}^{unif}$ such that $I[p] \leq \iota$. Letting $X^{(1)}, ..., X^{(k)} \sim \text{Unif}[0, 1]$, and $Y \sim \text{Unif}[0, 1]$ define $Z_i(y) = p(y|X_i)$. We have $\mathbf{E}(Z(y)) = 1$ and,

$$I[p(x, y)] = \mathbf{E}(Z(Y) \log Z(Y))$$

while

$$\text{ABA}_k[p(x, y)] = k^{-1} \mathbf{E}(\max_i Z_i(Y)).$$

Letting G_y be the distribution of $Z(y)$, we have

$$E[G_y] = 1$$

$$I[p(x, y)] = \mathbf{E}(I[G_Y])$$

$$\text{ABA}_k[p(x, y)] = \mathbf{E}(\psi_k[G_Y])$$

where the expectation is taken over $Y \sim \text{Unif}[0, 1]$ and where $E[G]$, $I[G]$, and $\psi_k[G]$ are defined as in Lemma **??**.

Define the random variable $J = I[G_Y]$. We have

$$\begin{aligned} \text{ABA}_k[p(x, y)] &= \mathbf{E}(\psi_k[G_Y]) \\ &= \int_0^1 \psi_k[G_y] dy \\ &\leq \int_0^1 \left(\sup_{G: I[G] \leq I[G_y]} \psi_k[G] \right) dy \\ &= \int_0^1 f(I[G_y]) dy = \mathbf{E}[f(J)]. \end{aligned}$$

Now, since f is concave by Lemma **??**, we can apply Jensen's inequality to conclude that

$$\text{ABA}_k[p(x, y)] = \mathbf{E}[f(J)] \leq f(\mathbf{E}[J]) = f(\iota),$$

which completes the proof. $\square$

4.4 Lower confidence bound

Get lower confidence bound for ABA then plug into result.

4.5 Example

Chapter 5

High-dimensional inference of mutual information

5.1 Motivation

5.1.1 Quantifying precision of decoding models

Both computational and cognitive neuroscience are concerned with understanding brain function: while computational neuroscience is concerned with understanding functionality at the level of the spiking behavior of individual neurons and small neural populations, cognitive neuroscience tends to emphasize functionality at the level of macroscale regions of the interest in the brain. While the recording technologies, motivating questions, and analytical methodologies differ between the two subdisciplines, the conceptualization of brain functionality in terms of *encoding* and *decoding* models has been widely applied in both areas Quian Quiroga and Panzeri 2009Naselaris et al. 2011. In computational neuroscience, cell recording experiments are conducted to determine whether spike trains have a temporal and/or correlational code Nelken et al. 2005Hatsopoulos et al. 1998, to examine how the neural code adapts to changes in stimulus distribution Fairhall et al. 2001 and whether downstream neurons make use of higher-order correlations for decoding Oizumi et al. 2010. Meanwhile, in neuroimaging studies, functional MRI experiments are employed to model the receptive fields of early visual areas in the human brain Kay et al. 2008, to examine the semantic encoding of words Mitchell et al. 2008 or objects Huth et al. 2012.

The dual perspectives of encoding and decoding originate naturally from the fact that in examining the link between brain activity and function, one can either start with brain activity on one end, or with external stimulation or behavioral observation on the other end. Starting by exposing the subject to sensory stimuli or prompting the subject to engage in particular motor tasks, one can search for areas in the brain which respond to the task: in other words, one can test to see which areas of the brain *encode* the given stimulus. In the other direction, one seeks to understand the functionality of a given brain region: in other words, how to *decode* brain activity in that region.

Formulation of encoding models is relatively straightforward, since one needs only to characterize the observed brain response to a given stimulus. One can further ask how to distinguish between signal and noise in the encoding mechanism Nelken et al. 2005, or in complex stimuli, seek a linearizing feature set which reveals the nature of the brain representation Naselaris et al. 2011. However, the establishment of complete decoding models is much less amenable to experiemental manipulation, since to exhaustively characterize the functionality of a neuron, one would

have to know in advance the type of information it encodes. Early advances in decoding often depended on strokes of luck: Hubel Hubel 1982 originally discovered the existence of neurons with orientation-sensitive receptive fields due to the vigorous response of a cell to the perfectly angled shadow of a glass slide that they were inserting into the ophthalmoscope. Yet, even now, the goal of completely characterizing the function of a given brain region remains a difficult task, with the most promising approach being a *reverse inference* procedure Poldrack 2006 which aggregates information from the literature about activity-functionality relationships.

A more feasible goal is to establish the *precision* with which a neuron can decode a particular type of feature. This can be accomplished by first training an encoding model, and then inverting the encoding model using Bayes' rule to obtain a decoding model Oram et al. 1998aQuian Quiroga and Panzeri 2009Naselaris et al. 2011.

By decoding *precision*, we mean the specificity which we can identify or reconstruct the stimulus based on the neural response. As such, in our view, the term decoder *precision* is more or less synonymous with terms such as decoder *performance* or decoder *accuracy* as they are used in the literature. However, we choose the word *precision* in particular, because it communicates the idea that the essential quality of a good decoder is that it allows one to confidently and precisely infer the stimulus.

Measures of decoding precision can be used to support several different kinds of scientific inferences. When there exist multiple plausible encoding models–for instance, a model where stimulus information is encoded solely by average firing rate versus a model where inter-spike timings also carry information–the precision of the decoder can be used as a basis for deciding the best encoding model. For two encoding models with equal complexity, such as comparing two different types of receptive field models, the model with better decoding precision could be considered the more plausible model. In the case where a more complex encoding model is compared to a strictly simpler model–such as comparing a model with a temporal code versus a model only incorporating average firing rate, a substantial improvement in decoding precision for the more complex model is needed to demonstrate its validity, since in the null hypothesis where the simpler model is correct, the more complex model should still have approximately equal decoding performance.

Yet another application of decoding precision is to track the adaptivity of the neural code. Fairhall Fairhall et al. 2001 recorded the output of a motion-sensitive neuron in a fly in response to a visual stimulus with changing angular velocity. Changing the variance of the stimulus results in rapid adaptation: the neural code starts adapting to the change in stimulus distribution within tens of milliseconds, which is reflected by an increased or decreased precision (as measured by mutual information) in resolving angular velocity to match the variance of the stimulus. More generally, comparisons of decoding precisions between different conditions can show how the encoded information increases or decreases across experimental conditions. Kayser Kayser, Logothetis, and Panzeri 2010 demonstrated how the mutual information between a sound stimulus and neurons in the auditory cortex increased when the subjects were also presented a matching visual stimulus (e.g. showing a picture of a lion roaring while playing the sound of a lion's roar.)

Differing types and parameterizations of stimuli naturally lead to differing measures of decoding precision. For stimuli which can be parameterized by a scalar x, the precision can be measured by the squared correlation coefficient R^2 Abbott 1994. However, the resulting measure of precision is not invariant to scaling of the parameterization: for instance, the choice of whether to parameterize volume on an absolute scale or a logarithmic scale. The mutual information Shannon 1948 between the stimulus and the predicted stimulus is invariant to the parameterization of the

stimulus. Due to its invariance and a number of other properties, the mutual information is widely used to measure the precision of the neural code in cell recording studies, both for single-neuron decoding models Borst and Theunissen 1999 and for population coding models Quian Quiroga and Panzeri 2009Ince et al. 2010.

However, the difficulties of estimating mutual information in small samples has been widely recognized, with a large literature on bias correction methods Panzeri et al. 2007Paninski 2003. Methods for bias correction have been developed for three different sample size regimes: the moderate-sample regime, where the number of observations is larger than the number of stimulus-response pairsMiller 1955Strong et al. 1998Treves and Panzeri 1995, the undersampled regime, where the number of observations is less than the number of stimulus-response pairs Nemenman, Bialek, and de Ruyter van Steveninck 2004, and a *stimulus-undersampled* regime, where only a small fraction of possible stimuli are sampled, but with a large number of observations for each of the sampled stimuli Gastpar, Gill, and Theunissen 2009. Nevertheless, even the bias-corrected estimates may be unusably inaccurate in problems of moderate dimensionality, since the cardinality of response space grows exponentially with the dimensionality. In such cases, alternative approaches for estimating the mutual information include the assumption of a parametric model Brunel and Nadal 1998Gastpar, Gill, and Theunissen 2009Yarrow, Challis, and Seriès 2012, or usage of the maximum entropy principle to obtain bounds on the mutual information subject to the empirical moments of a certain order Ince et al. 2009Globerson et al. 2009.

Perhaps due to the technical difficulties of estimating mutual information in high dimensions, mutual information has never, to our knowledge, been used as a measure of decoding precision in neuroimaging studies, although it has been proposed for the purpose of bypassing the modelling of the hemodynamic response function for single-voxel analyses Fuhrmann Alpert et al. 2007. Instead, a variety of methods are employed to characterize the precision of decoding models, depending on the nature of the stimulus and the experimental setup.

In task fMRI experiments where stimuli are drawn from a number of disjoint semantic categories– for instance, 'birds', 'insects', and 'mammals' as in Connolly et al. 2012, it is natural to construct a decoder which outputs the predicted category of a stimulus as a function of the response. Such a decoder is known as a *classifier* in the machine learning literature Hastie, Tibshirani, and Friedman 2009, and a natural measure of classifier precision is the probability that the decoder outputs the correct category on a new, randomly drawn test example, which is the *classification accuracy*.

In experiments where the subject is presented a number of parameterized stimuli are drawn from a continuous distribution (such as natural images or sounds), there are two types of decoders which can be constructed. In the first case, one constructs a decoder which estimates the parameters of the stimulus which we call a *reconstructor*: the precision of such a decoder is measured by the correlation between the estimated and true parameter vector Pasley et al. 2012 Nishimoto et al. 2011Naselaris et al. 2009. In the second case, one constructs a decoder which picks the most likely stimulus from a finite library of examples *which includes the true stimulus* Kay et al. 2008Mitchell et al. 2008. Since the true stimulus is included in the library, the task is to 'identify' the correct stimulus from the library. A natural measure of decoder performance is therefore the probability of correct identification. However, note that this probability is dependent on the arbitrary choice of the size of the exemplar library: a different choice for library size therefore results in a different measure of precision. We refer to the probability of correct classification for a library of k exemplars as the *k-example identification accuracy*.

In their respective domains, these different measures of precision suffice to make inferences on many interesting scientific questions: to list a few examples, showing the superiority of a Gabor filters versus center-surround filters for modeling the receptive fields of V1 and V2 neurons Kay et al. 2008, or demonstrating that brain activity in response to viewing an Engish noun can be predicted from word association frequencies Mitchell et al. 2008.

A commonality to all applications of decoding models in neuroimaging is the pairwise comparison of two decoding models (Gabor vs. retinotopic) or the comparison of a single decoding model to chance accuracy. Looking ahead to anticipate what kinds of analyses might be employed in the future based on neuroimaging data, it is suggestive to note that the earliest decoding studies in the cell recording literature also involved comparisons between two or three different decoders Eckhorn et al. 1976. However, as neuroscientists began to consider questions of population coding, analyses of the redundancy between neurons started to make use of comparisons between large numbers of decoders: for a population of N neurons, one might compare the precision of a decoder (mutual information) based on the entire ensemble, compared to the precisions of decoders based on each of the N individual neurons. Furthermore, one can make the same comparison for a range of different ensemble sizes N. As questions about the redundancy of the neural code are relevant on both the micro scale (the domain of cell recording studies) and the macro scale (the domain of neuroimaging), it is safe to assume that similar analyses, requiring comparisons of large numbers of decoders, will emerge in neuroimaging studies. Already in the functional MRI literature, we see similar decompositions of decoding accuracy versus ensemble size Kay et al. 2008, but another possible type of decomposition would be to compare decoding performance as the number of stimulus features is varied, rather than the number of voxels.

The scaling properties of mutual information are highly advantageous when comparing multiple decoders, which could potentially span a wide range of decoding precision: for instance, a single neuron versus an ensemble of thousands of neurons. In contrast, classification accuracy, k-class identification accuracy and reconstruction accuracy all suffer from the issue of *limited dynamic range*: that is, they are only effective at measuring precision within a certain range.

Let us illustrate with the example of identification accuracy. A low precision decoder, such as a decoder based on a single voxel, may have an accuracy which is so close to chance accuracy, $1/k$, as to be statistically indistinguishable from chance based on the data. On the other hand, a sufficiently high-precision decoder may face the opposite problem, where it achieves perfect classification on the limited number of test examples. Any empirical estimate of identification accuracy can only be used to accurately rank decoders which have accuracies sufficiently bounded away from both $1/k$ and 1. The same issue applies to reconstruction accuracy (bounded between 0 and 1) and classification accuracy (bounded between $1/k$ and 1, where k is the number of classes): any bounded measure of precision is ineffective at comparing decoders which are too close to either the upper bound or lower bound of achievable precision.

In practice, the solution to this issue is to find a measure of precision which is well-suited for all of the decoders that needed to be compared. If there are two encoding models which both achieve perfect classification on the test set, then perhaps the more demanding measure of reconstruction accuracy can be used to distinguish them. However, this strategy begins to become impractical as the number of decoders to be compared increases. One wishes to relate the decoding precision of an N-voxel ensemble for N spanning from 1 to 10000: however, any bounded measure

of precision which is suitably stringent for distinguishing $N = 9999$ from $N = 10000$ would fail for comparing $N = 1$ to $N = 2$, and vice-versa.

We have seen that one solution to this predicament is to use an unbounded measure of precision which can remain sensitive to variations in precision across a large dynamic range: for instance, the mutual information. Yet, given the difficulty of estimating the mutual information in high-dimensional settings, one might consider another approach: to develop a systematic means for comparing decoders by using multiple (easily estimated) precision measures, each of which may only capture a limited range of precisions, but which collectively span a sufficiently large range of precisions to include all of the decoders being compared.

Our contribution in this paper is to show that both of these approaches–the estimation of mutual information, and the comparison of decoders based on a range of decoding metrics, turn out to be the very same problem in high-dimensional settings. The *identification accuracy curve*, which we define as the collection of all k-class identification accuracies for $k \geq 2$, can be used to compare a collection of decoders over a large span of precisions. Yet, a recent theoretical resultZheng and Benjamini 2016 shows that the identification accuracy curve for the Bayes decoder (the optimal decoder) is determined by the mutual information in a certain high-dimensional regime. While it is generally not feasible to approximate the Bayes decoder in high-dimensional settings, we use this result to define the *implied information* for a non-Bayes (suboptimal) decoder. The implied information, $I_{implied}$, is not the true mutual information between the stimulus and response, but it provides a means of comparing two accuracy curves (estimate the implied information from each, and then compare the estimates), as well as providing an unbounded measure of decoding precision which, similar to mutual information, has desirable scaling properties for the purpose of comparing decoders spanning a range of precisions.

5.1.2 Kay et al. example

5.2 Setup

The theory applies to a high-dimensional limit where $I(X;Y)$ tends to a constant.

A1. $\lim_{d \to \infty} I(X^{[d]}; Y^{[d]}) = \iota < \infty$.

A2. There exists a sequence of scaling constants $a_{ij}^{[d]}$ and $b_{ij}^{[d]}$ such that the random vector $(a_{ij}\ell_{ij}^{[d]} + b_{ij}^{[d]})_{i,j=1,...,k}$ converges in distribution to a multivariate normal distribution, where $\ell_{ij} = \log p(y^{(i)}|x^{(i)})$ for independent $y^{(i)} \sim p(y|x^{(i)})$.

A3. Define
$$u^{[d]}(x, y) = \log p^{[d]}(x, y) - \log p^{[d]}(x) - \log p^{[d]}(y).$$

There exists a sequence of scaling constants $a^{[d]}$, $b^{[d]}$ such that

$$a^{[d]} u^{[d]}(X^{(1)}, Y^{(2)}) + b^{[d]}$$

converges in distribution to a univariate normal distribution.

A4. For all $i \neq k$,

$$\lim_{d \to \infty} \text{Cov}[u^{[d]}(X^{(i)}, Y^{(j)}), u^{[d]}(X^{(k)}, Y^{(j)})] = 0.$$

Assumptions A1-A4 are satisfied in a variety of natural models. One example is a multivariate Gaussian sequence model where $X \sim N(0, \Sigma_d)$ and $Y = X + E$ with $E \sim N(0, \Sigma_e)$, where Σ_d and Σ_e are $d \times d$ covariance matrices, and where X and E are independent. Then, if $d\Sigma_d$ and Σ_e have limiting spectra H and G respectively, the joint densities $p(x, y)$ for $d = 1, \ldots$, satisfy assumptions A1 - A4. Another example is the multivariate logistic model, which we describe in section 3. We further discuss the rationale behind A1-A4 in the supplement, along with the detailed proof.

5.3 Theory

We obtain the universality result in two steps. First, we link the average Bayes error to the moments of some statistics Z_i. Secondly, we use taylor approximation in order to express $I(X; Y)$ in terms of the moments of Z_i. Connecting these two pieces yields the formula (**??**).

Let us start by rewriting the average Bayes error:

$$e_{ABE,k} = \Pr[p(Y|X_1) \leq \max_{j \neq 1} p(Y|X_j)|X = X_1].$$

Defining the statistic $Z_i = \log p(Y|X_i) - \log p(Y|X_1)$, where $Y \sim p(y|X_1)$, we obtain $e_{ABE} = \Pr[\max_{j>1} Z_i > 0]$. The key assumption we need is that $Z_2, \ldots, Z_k$ are asymptotically multivariate normal. If so, the following lemma allows us to obtain a formula for the misclassification rate.

Lemma 1. *Suppose $(Z_1, Z_2, \ldots, Z_k)$ are jointly multivariate normal, with $\mathbf{E}[Z_1 - Z_i] = \alpha$, $Var(Z_1) = \beta \geq 0$, $Cov(Z_1, Z_i) = \gamma$, $Var(Z_i) = \delta$, and $Cov(Z_i, Z_j) = \epsilon$ for all $i, j = 2, \ldots, k$, such that $\beta + \epsilon - 2\gamma > 0$. Then, letting*

$$\mu = \frac{\mathbf{E}[Z_1 - Z_i]}{\sqrt{\frac{1}{2} Var(Z_i - Z_j)}} = \frac{\alpha}{\sqrt{\delta - \epsilon}},$$

$$\nu^2 = \frac{Cov(Z_1 - Z_i, Z_1 - Z_j)}{\frac{1}{2} Var(Z_i - Z_j)} = \frac{\beta + \epsilon - 2\gamma}{\delta - \epsilon},$$

we have

$$\Pr[Z_1 < \max_{i=2}^{k} Z_i] = \Pr[W < M_{k-1}]$$

$$= 1 - \int \frac{1}{\sqrt{2\pi\nu^2}} e^{-\frac{(w-\mu)^2}{2\nu^2}} \Phi(w)^{k-1} dw,$$

where $W \sim N(\mu, \nu^2)$ and M_{k-1} is the maximum of $k - 1$ independent standard normal variates, which are independent of W.

To see why the assumption that $Z_2, \ldots, Z_k$ are multivariate normal might be justified, suppose that X and Y have the same dimensionality d, and that joint density factorizes as

$$p(x^{(j)}, y) = \prod_{i=1}^{d} p_i(x_i^{(j)}, y_i)$$

where $x_i^{(j)}, y_i$ are the ith scalar components of the vectors $x^{(j)}$ and y. Then,

$$Z_i = \sum_{m=1}^{d} \log p_m(y_m|x_m^{(i)}) - \log p_m(y_m|x_1^{(m)})$$

where $x_{i,j}$ is the ith component of x_j. The d terms $\log p_m(y_m|x_{m,i}) - \log p_m(y_m|x_{m,1})$ are independent across the indices m, but dependent between the $i = 1, \ldots, k$. Therefore, the multivariate central limit theorem can be applied to conclude that the vector $(Z_2, \ldots, Z_k)$ can be scaled to converge to a multivariate normal distribution. While the componentwise independence condition is not a realistic assumption, the key property of multivariate normality of $(Z_2, \ldots, Z_k)$ holds under more general conditions, and appears reasonable in practice.

It remains to link the moments of Z_i to $I(X; Y)$. This is accomplished by approximating the logarithmic term by the Taylor expansion

$$\log \frac{p(x,y)}{p(x)p(y)} \approx \frac{p(x,y) - p(x)p(y)}{p(x)p(y)} - \left(\frac{p(x,y) - p(x)p(y)}{p(x)p(y)}\right)^2 + \ldots.$$

A number of assumptions are needed to ensure that needed approximations are sufficiently accurate; and additionally, in order to apply the central limit theorem, we need to consider a *limiting sequence* of problems with increasing dimensionality. We now state the theorem.

Theorem 1. *Let $p^{[d]}(x,y)$ be a sequence of joint densities for $d = 1, 2, \ldots$. Further assume that*

A1. $\lim_{d\to\infty} I(X^{[d]}; Y^{[d]}) = \iota < \infty$.

A2. *There exists a sequence of scaling constants $a_{ij}^{[d]}$ and $b_{ij}^{[d]}$ such that the random vector $(a_{ij}\ell_{ij}^{[d]} + b_{ij}^{[d]})_{i,j=1,\ldots,k}$ converges in distribution to a multivariate normal distribution, where $\ell_{ij} = \log p(y^{(i)}|x^{(i)})$ for independent $y^{(i)} \sim p(y|x^{(i)})$.*

A3. *Define*
$$u^{[d]}(x,y) = \log p^{[d]}(x,y) - \log p^{[d]}(x) - \log p^{[d]}(y).$$

There exists a sequence of scaling constants $a^{[d]}$, $b^{[d]}$ such that

$$a^{[d]}u^{[d]}(X^{(1)}, Y^{(2)}) + b^{[d]}$$

converges in distribution to a univariate normal distribution.

A4. *For all $i \neq k$,*
$$\lim_{d\to\infty} Cov[u^{[d]}(X^{(i)}, Y^{(j)}), u^{[d]}(X^{(k)}, Y^{(j)})] = 0.$$

Then for $e_{ABE,k}$ as defined above, we have

$$\lim_{d\to\infty} e_{ABE,k} = \pi_k(\sqrt{2\iota})$$

where

$$\pi_k(c) = 1 - \int_{\mathbb{R}} \phi(z-c)\Phi(z)^{k-1}dz$$

where ϕ and Φ are the standard normal density function and cumulative distribution function, respectively.

5.4 Estimator

Define the Bayes risk as the identification risk of the optimal decoder. The result of ZB 2016 says that under certain regularity conditions, for for sufficiently high-dimensional $p(\vec{x}, \vec{y})$, we have

$$\text{BayesAcc}_k \approx \bar{\pi}_k(\sqrt{2I(\vec{x}; \vec{y})})$$

where $\bar{\pi}_k$ is the function

$$\bar{\pi}_k(c) = \int_{\mathbb{R}} \phi(z - c)\Phi(z)^{k-1}dz.$$

and where $I(\vec{x}; \vec{y})$ is the Shannon information

$$I(\vec{X}; \vec{Y}) = \int p(\vec{x}, \vec{y}) \log \frac{p(\vec{x}, \vec{y})}{p(\vec{x})p(\vec{y})} dx dy.$$

This is an important result because it implies that the entire identification accuracy curve can be summarized by a single parameter–the mutual information. This means that in the asymptotic regime specified by ZB 2016, (i) any portion of the curve can be used to estimate the mutual information and therefore reconstruct the entire curve, and (ii) that there exists a strict ordering over identification accuracy curves: for any two curves A_k and A'_k, one dominates the other for all k: either $A_k \geq A'_k$ for all $k \geq 2$, or $A'_k \geq A_k$ for all $k \geq 2$.

However, the result in ZB 2016 only applies to the optimal decoder, or *Bayes decoder*. Yet, it is impossible to obtain the Bayes decoder in practice, since constructing the Bayes decoder requires knowing $p(\vec{x}, \vec{y})$. Therefore, we propose that under similar conditions to those stipulated in ZB 2016, for a certain class of classifiers[1], we have

$$\text{IdAcc}_k \approx \bar{\pi}_k(\sqrt{2I_{implied}})$$

where IdRisk_k is the k-class identification risk for a given classifier trained from the training set, and where $I_{implied}$ is a real-valued attribute of the classifier called the *implied information*. Furthermore, since $\text{IdAcc}_k \leq \text{BayesAcc}_k$ by definition (as BayesAcc_k is the best achievable accuracy), we have

$$I_{implied} \leq I(\vec{X}; \vec{Y}).$$

In order to estimate the implied information, we can rely on the fact that the empirical identification accuracy curve EmpAcc_k is an unbiased estimate of the true identification accuracy curve IdAcc_k. Therefore, we can estimate $I_{implied}$ by finding the theoretical curve which gives the best fit to the empirical accuracies in terms of mean-squared error. Thus, define $\hat{I}_{implied}$ as the nonlinear least-squares estimator

$$\hat{I}_{implied} = \text{argmin}_{\iota \geq 0} \sum_{k=2}^{M} (\text{EmpAcc}_k - \bar{\pi}_k(\sqrt{2\iota}))^2.$$

5.5 Examples

---

[1]We leave it to future work to specify the conditions on the joint density and classifiers needed to formally establish the desired property.

Appendix A

Frequently Asked Questions

A.1 How do I change the colors of links?

The color of links can be changed to your liking using:
    `\hypersetup{urlcolor=red}`, or
    `\hypersetup{citecolor=green}`, or
    `\hypersetup{allcolor=blue}`.
If you want to completely hide the links, you can use:
    `\hypersetup{allcolors=.}`, or even better:
    `\hypersetup{hidelinks}`.
If you want to have obvious links in the PDF but not the printed text, use:
    `\hypersetup{colorlinks=false}`.

Bibliography

Abbott, Larry F. (1994). "Decoding neuronal firing and modelling neural networks." In: *Quarterly reviews of biophysics* 27.3, pp. 291–331. ISSN: 0033-5835. URL: http://www.ncbi.nlm.nih.gov/pubmed/7899551.

Borst, Alexander and Frédéric E. Theunissen (1999). "Information theory and neural coding". In: *Nature Neuroscience* 2.11, pp. 947–957. ISSN: 10976256. DOI: 10.1038/14731. URL: http://www.nature.com/doifinder/10.1038/14731.

Brunel, Nicolas and J P Nadal (1998). "Mutual information, Fisher information, and population coding." In: *Neural computation* 10.7, pp. 1731–57. ISSN: 0899-7667. DOI: 10.1162/089976698300017115. arXiv: arXiv:1011.1669v3. URL: http://www.ncbi.nlm.nih.gov/pubmed/9744895.

Clarkson, Philip and Pedro J Moreno (1999). "On the use of support vector machines for phonetic classification". In: *Acoustics, Speech, and Signal Processing, 1999. Proceedings., 1999 IEEE International Conference on*. Vol. 2. IEEE, pp. 585–588.

Connolly, Andrew C. et al. (2012). "The Representation of Biological Classes in the Human Brain". In: *The Journal of neuroscience : the official journal of the Society for Neuroscience* 32.8, pp. 2608–2618. ISSN: 0270-6474. DOI: 10.1523/JNEUROSCI.5547-11.2012. URL: http://www.ncbi.nlm.nih.gov/pmc/articles/PMC3532035/{\%}5Cnhttp://www.ncbi.nlm.nih.gov/pmc/articles/PMC3532035/pdf/nihms361453.pdf.

Daniels, Michael J. and Robert E. Kass (2001). "Shrinkage Estimators for Covariance Matrices". In: *Biometrics* 57.4, pp. 1173–1184. ISSN: 0006341X. DOI: 10.1111/j.0006-341X.2001.01173.x. URL: http://doi.wiley.com/10.1111/j.0006-341X.2001.01173.x.

Deng, Jia et al. (2010). "What does classifying more than 10,000 image categories tell us?" In: *European conference on computer vision*. Springer, pp. 71–84.

Duygulu, Pinar et al. (2002). "Object recognition as machine translation: Learning a lexicon for a fixed image vocabulary". In: *European conference on computer vision*. Springer, pp. 97–112.

Eckhorn, R et al. (1976). "Efficiency of Different Neuronal Codes: Information Transfer Calculations for Three Different Neuronal Systems". In: *Biol. Cybernetics* 22, pp. 49–60.

Fairhall, Adrienne L. et al. (2001). "Efficiency and ambiguity in an adaptive neural code". In: *Nature* 412.23, pp. 787–792. ISSN: 0028-0836. DOI: 10.1038/35090500. URL: http://www.nature.com/doifinder/10.1038/35090500.

Fisher, Ronald A (1936). "The use of multiple measurements in taxonomic problems". In: *Annals of eugenics* 7.2, pp. 179–188.

Frey, Peter W and David J Slate (1991). "Letter recognition using Holland-style adaptive classifiers". In: *Machine learning* 6.2, pp. 161–182.

Fuhrmann Alpert, Galit et al. (2007). "Spatio-temporal information analysis of event-related BOLD responses". In: *NeuroImage* 34.4, pp. 1545–1561. ISSN: 10538119. DOI: 10.1016/j.neuroimage.2006.10.020.

Gastpar, Michael C., Patrick R. Gill, and Frédéric E. Theunissen (2009). "Anthropic correction of information estimates". In: *Proceedings - 2009 IEEE Information Theory Workshop on Networking and Information Theory, ITW 2009* 56.2, pp. 152–155. ISSN: 00189448. DOI: `10.1109/ITWNIT.2009.5158561`.

Globerson, Amir et al. (2009). "The minimum information principle and its application to neural code analysis." In: *Proceedings of the National Academy of Sciences of the United States of America* 106.9, pp. 3490–5. ISSN: 1091-6490. DOI: `10.1073/pnas.0806782106`. URL: `http://www.ncbi.nlm.nih.gov/pubmed/19218435http://www.pubmedcentral.nih.gov/articlerender.fcgi?artid=PMC2651257`.

Grother, Patrick J (1995). "NIST special database 19". In: *Handprinted forms and characters database, National Institute of Standards and Technology*.

Hastie, Trevor, Robert Tibshirani, and Jerome Friedman (2009). *The Elements of Statistical Learning*. 2nd ed. Vol. 1. Springer, pp. 337–387. ISBN: 9780387848570. DOI: `10.1007/b94608`. arXiv: `1010.3003`. URL: `http://www.springerlink.com/index/10.1007/b94608`.

Hatsopoulos, N G et al. (1998). "Information about movement direction obtained from synchronous activity of motor cortical neurons." In: *Proceedings of the National Academy of Sciences of the United States of America* 95.26, pp. 15706–11. ISSN: 0027-8424. URL: `http://www.ncbi.nlm.nih.gov/pubmed/9861034http://www.pubmedcentral.nih.gov/articlerender.fcgi?artid=PMC28108`.

Hubel, David H. (1982). "Evolution of ideas on the primary visual cortex, 1955–1978: A biased historical account". In: *Bioscience Reports* 2.7, pp. 435–469.

Huth, Alexander G. et al. (2012). "A Continuous Semantic Space Describes the Representation of Thousands of Object and Action Categories across the Human Brain". In: *Neuron* 76.6, pp. 1210–1224. ISSN: 08966273. DOI: `10.1016/j.neuron.2012.10.014`. arXiv: `NIHMS150003`.

Ince, Robin A A et al. (2009). "Python for information theoretic analysis of neural data." In: *Frontiers in neuroinformatics* 3, p. 4. ISSN: 1662-5196. DOI: `10.3389/neuro.11.004.2009`. URL: `http://www.ncbi.nlm.nih.gov/pubmed/19242557http://www.pubmedcentral.nih.gov/articlerender.fcgi?artid=PMC2647335`.

Ince, Robin A.A. et al. (2010). "Information-theoretic methods for studying population codes". In: *Neural Networks* 23.6, pp. 713–727. ISSN: 08936080. DOI: `10.1016/j.neunet.2010.05.008`.

Kay, Kendrick N et al. (2008). "Identifying natural images from human brain activity." In: *Nature* 452.March, pp. 352–355. ISSN: 0028-0836. DOI: `10.1038/nature06713`.

Kayser, Christoph, Nikos K. Logothetis, and Stefano Panzeri (2010). "Visual Enhancement of the Information Representation in Auditory Cortex". In: *Current Biology* 20.1, pp. 19–24. ISSN: 09609822. DOI: `10.1016/j.cub.2009.10.068`.

Ledoit, Olivier and Michael Wolf (2004). "Honey, I Shrunk the Sample Covariance Matrix". In: *The Journal of Portfolio Management* 30.4, pp. 110–119. ISSN: 0095-4918. DOI: `10.3905/jpm.2004.110`.

Mickalstd, RS (1980). "LEARNING BY BEING TOLD AND LEARNING FROM EXAMPLES: AN EXPERIMENTAL COMPARISON OF THE TWO METHODS OF KNOWLEDGE ACQUISITION". In:

Miller (1955). "Note on the bias of information estimates". In: *Information Theory in Psychology: Problems and Methods*.

Mitchell, Tom M. et al. (2008). "Predicting Human Brain Activity Associated with the Meanings of Nouns". In: *Science* 320.5880.

Naselaris, Thomas et al. (2009). "Bayesian Reconstruction of Natural Images from Human Brain Activity". In: *Neuron* 63.6, pp. 902–915. ISSN: 08966273. DOI: 10.1016/j.neuron.2009.09.006. URL: http://dx.doi.org/10.1016/j.neuron.2009.09.006.

Naselaris, Thomas et al. (2011). "Encoding and decoding in fMRI". In: *NeuroImage* 56.2, pp. 400–410. ISSN: 10538119. DOI: 10.1016/j.neuroimage.2010.07.073. URL: http://dx.doi.org/10.1016/j.neuroimage.2010.07.073.

Nelken, Israel et al. (2005). "Encoding Stimulus Information by Spike Numbers and Mean Response Time in Primary Auditory Cortex". In: *Journal of Computational Neuroscience* 19, pp. 199–221.

Nemenman, Ilya, William Bialek, and Rob de Ruyter van Steveninck (2004). "Entropy and information in neural spike trains: progress on the sampling problem." In: *Physical review. E, Statistical, nonlinear, and soft matter physics* 69.5 Pt 2, p. 056111. ISSN: 1539-3755. DOI: 10.1103/PhysRevE.69.056111. arXiv: 0306063 [physics]. URL: http://www.ncbi.nlm.nih.gov/pubmed/15244887http://link.aps.org/doi/10.1103/PhysRevE.69.056111.

Nishimoto, Shinji et al. (2011). "Reconstructing visual experiences from brain activity evoked by natural movies". In: *Current Biology* 21, pp. 1641–1646. ISSN: 09609822. DOI: 10.1016/j.cub.2011.08.031.

Oizumi, Masafumi et al. (2010). "Mismatched Decoding in the Brain". In: *Journal of Neuroscience* 30.13, pp. 4815–1826.

Oram, Mike W. et al. (1998a). "The 'Ideal Homunculus': decoding neural population signals". In: *Trends in Neurosciences* 21.6, pp. 259–265. ISSN: 01662236. DOI: 10.1016/S0166-2236(97)01216-2.

Oram, Mike W et al. (1998b). "TheIdeal Homunculus': decoding neural population signals". In: *Trends in neurosciences* 21.6, pp. 259–265.

Paninski, Liam (2003). "Estimation of Entropy and Mutual Information". In: *Neural Computation* 15.6, pp. 1191–1253. ISSN: 0899-7667. DOI: 10.1162/089976603321780272. arXiv: 0402594v3 [arXiv:cond-mat]. URL: http://www.mitpressjournals.org/doi/abs/10.1162/089976603321780272.

Panzeri, Stefano et al. (2007). "Correcting for the Sampling Bias Problem in Spike Train Information Measures". In: *Journal of Neurophysiology* 98.3.

Partalas, Ioannis et al. (2015). "LSHTC: A benchmark for large-scale text classification". In: *arXiv preprint arXiv:1503.08581*.

Pasley, Brian N. et al. (2012). "Reconstructing speech from human auditory cortex". In: *PLoS Biology* 10.1. ISSN: 15449173. DOI: 10.1371/journal.pbio.1001251.

Poldrack, Russell A. (2006). "Can cognitive processes be inferred from neuroimaging data?" In: *Trends in Cognitive Sciences* 10.2, pp. 59–63. ISSN: 13646613. DOI: 10.1016/j.tics.2005.12.004.

Quian Quiroga, Rodrigo and Stefano Panzeri (2009). "Extracting information from neuronal populations: information theory and decoding approaches." In: *Nature reviews. Neuroscience* 10.3, pp. 173–185. ISSN: 1471-003X. DOI: 10.1038/nrn2578.

Shannon, C. E. (1948). "A Mathematical Theory of Communication". In: *Bell System Technical Journal* 27.3, pp. 379–423. ISSN: 00058580. DOI: 10.1002/j.1538-7305.1948.tb01338.x. URL: http://ieeexplore.ieee.org/lpdocs/epic03/wrapper.htm?arnumber=6773024.

Strong, S. P. et al. (1998). "Entropy and Information in Neural Spike Trains". In: *Physical Review Letters* 80.1, pp. 197–200. ISSN: 0031-9007. DOI: 10.1103/PhysRevLett.80.197.

Treves, Alessandro and Stefano Panzeri (1995). "The Upward Bias in Measures of Information Derived from Limited Data Samples". In: *Neural Computation* 7.2, pp. 399–407. ISSN: 0899-7667. DOI: 10.1162/neco.1995.7.2.399.

Yarrow, Stuart, Edward Challis, and Peggy Seriès (2012). "Fisher and Shannon Information in Finite Neural Populations". In: *Neural Computation* 24.7, pp. 1740–1780. ISSN: 0899-7667. DOI: 10.1162/NECO_a_00292.

Zheng, Charles Y. and Yuval Benjamini (2016). "Estimating mutual information in high dimensions via classification error". In: arXiv: 1606.05229. URL: http://arxiv.org/abs/1606.05229.

Zou, Hui and Trevor Hastie (2005). "Regularization and variable selection via the elastic net". In: *Journal of the Royal Statistical Society: Series B (Statistical Methodology)* 67.2, pp. 301–320. ISSN: 1369-7412. DOI: 10.1111/j.1467-9868.2005.00503.x. URL: http://doi.wiley.com/10.1111/j.1467-9868.2005.00503.x.